Aus dem Institut für Biochemie
der Medizinischen Fakultät Charité – Universitätsmedizin Berlin

DISSERTATION

Targeting proteolysis in viral cardiac inflammatory disease

Einfluss der Proteolyse auf Virus-assoziierte entzündliche Herzmuskelerkrankungen

zur Erlangung des akademischen Grades
Doctor medicinae (Dr. med.)

vorgelegt der Medizinischen Fakultät
Charité – Universitätsmedizin Berlin

von

Hannah Louise Neumaier

Datum der Promotion: 30.11.2023

Table of contents

List of figures and tables

List of abbreviations

3-R guidelines	animal welfare guidelines: replacement, reduction, refinement
A/J	inbred mouse strain
CCL2/4	CC chemokine ligand 2/4
cDNA	complementary desoxyribonucleic acid
CVB3	Coxsackievirus B3
CXCL10	C-X-C motif chemokine 10
C57BL/6J	inbred mouse strain
ECG	electrocardiography
EDTA	ethylenediaminetetraacetic acid
FACS	flowcytometric
HeLa cells	human epithelial cell line (cervix carcinoma cells isolated from *He*nrietta *La*cks)
HEPES	(4-(2-hydroxyethyl)-1-piperazineethanesulfonic acid
ICI	immune checkpoint inhibitor
IL-1ß/-6	interleukin 1ß/-6
IFIT 1/3	interferon inducible
IFNb/g	interferon b/g
IP	immunoproteasome
LMP 2/7	low molecular protein 2/7
MECL-1	multicatalytic endopeptidase complex subunit
MHC	major histocompatibility
MLV reverse transcriptase	murine leukemia virus reverse transcriptase
mHPRT	murine hypoxanthine guanine phosphoribosyltransferase
MTT-stain	(3-(4,5-Dimethylthiazol-2-yl)
NMRI	outbred mouse strain
PBS	phosphate-buffered saline

Pen/Strep	Penicillin/Streptomycin
qPCR	quantitative polymerase chain reaction
RNA	ribonucleic acid
RPMI	growth medium for cell culture
TNFa	tumor necrosis factor a
UPS	ubiquitin proteasome system

German Summary

Proteolyse ist ein intrazellulärer Prozess, der durch die Aktivität des Proteasoms – eines multienzymatischen Komplexes – zur Aufrechterhaltung der intrazellulären Proteinhomöostase beiträgt und von dem zahlreiche Vorgänge abhängig sind. So werden Antigenpräsentation, intrazelluläre Kommunikationswege, Proteinqualitätskontrollen sowie Signale im Zellzyklus über die Funktionalität des Proteasoms reguliert.

Die Bildung einer Proteasomisoform, die überwiegend in Immunzellen exprimiert wird, des Immunoproteasoms (IP), kann durch genetisches Knockout oder einen spezifischen Inhibitor wie ONX 0914 blockiert werden. Da die Expression des IP im Rahmen entzündlicher Herzmuskelerkrankungen im Mausmodell in infiltrierenden Immunzellen wie auch Kardiomyozyten stark hochreguliert ist, eignen sich diese Modelle, um den Einfluss des IPs auf die Entzündungsreaktion zu untersuchen.

Obwohl das IP exprimiert wird, um die Proteinhomöostase einer Zelle in Phasen vermehrten zellulären Stresses intakt zu halten, kann diese Regulierung zu einer überschießenden Immunantwort mit chronischer Inflammation führen, woraus sich die Frage ergibt, ob die durch das IP mitverantwortete Entzündungsreaktion hilfreich oder vielmehr schädlich ist.

Wir infizierten Mäuse in einem Modell mit Coxsackievirus B3 (CVB3), das für die Untersuchung der akuten viralen Myokarditis gut charakterisiert ist. Eine Behandlung mit ONX 0914 oder dem Vehikel ermöglicht einen genaueren Blick auf entzündliche Prozesse und ihre Abhängigkeit vom IP.

Zuvor konnten wir zeigen, dass die akute CVB3-Myokarditis bei Mäusen, die ONX 0914 erhalten, signifikant gemildert wird – sie weisen verbessertes Gesamtüberleben auf und das Niveau der Entzündungsreaktion war deutlich reduziert.

Ziel dieses Projektes war, die präventiven und therapeutischen Möglichkeiten einer Hemmung der IP-Aktivität im Modell der CVB3-Myokarditis zu charakterisieren und eine schützende Wirkung sowohl im akuten als auch im chronischen Stadium der Krankheit zu untersuchen. Durchflusszytometrische und qPCR-Analysen von Herz- und Milzgewebe sowie Blutuntersuchungen ergaben, dass Mäuse eine höhere Viruslast, höhere virale Zytotoxizität und eine erhöhte Menge an Herzmuskel-infiltrierenden Immunzellen aufwiesen, wenn ihre IP-Funktion vor der Infektion durch ONX 0914 gehemmt wurde. Dies deutete auf einen Vorteil einer aufrechterhaltenen im

Gegensatz zur beeinträchtigten IP-Funktion in diesem Modell hin und veranlasste Untersuchungen der Wirksamkeit von ONX 0914 auf die Proteinexpression. Interessanterweise konnten wir in Experimenten, in denen das IP gehemmt wurde, nachdem Mäuse bereits mit CVB3 infiziert worden waren, keine schädliche Wirkung der Behandlung mit ONX 0914 nachweisen, was darauf hindeutet, dass die Schlüsselrolle des IPs während der Entzündungsreaktion in Frühstadien der Immunantwort liegt und die Frage aufwirft, ob eine Blockade des IPs andere proinflammatorische Kompensationsmechanismen verstärken könnte.

Abstract

Proteolysis, facilitated through activity of the proteasome – a multi-enzymatic complex – has numerous important purposes within a cells' protein homeostasis. The proteolytic machinery regulates antigen presentation, the activity of intracellular pathways, protein quality control and cell cycle signaling.

An isoform, predominantly expressed in immune cells and thus called the immunoproteasome can be targeted by genetic knockout or application of a specific inhibitor, such as ONX 0914, rendering it dysfunctional.

The immunoproteasomes' role has long been investigated in mouse models for cardiac inflammatory disease, as it is abundantly expressed in infiltrating immune cells as well as strongly upregulated in inflamed cardiomyocytes. While this isoform is expressed in aid of keeping a cells' protein balance intact under conditions of increased cellular stress, mouse models with a genetically predisposed background who develop acute viral myocarditis are prone to overwhelming inflammation and subsequent cardiac tissue damage, calling into question whether the inflammatory response is helpful or rather detrimental.

Here, mice are infected with Coxsackievirus B3 (CVB3) in a model that is well characterized for CVB3-induced acute and chronic viral myocarditis. Treatment with ONX 0914 or its vehicle only, allows a closer look at inflammatory processes and their dependence the immunoproteasome.

Previously, we found that CVB3-myocarditis can be significantly mitigated in mice receiving ONX 0914, improving overall survival and dampening the height of inflammatory response to the infection.

In this project, our objective was to follow up on the preventative and therapeutic capacity for ONX 0914, investigating a possible mitigating effect on viral cardiac inflammatory disease. We aimed to distinguish further the role of immunoproteasome-specific inhibition during both acute and chronic stages of the disease. Flow cytometric and qPCR analysis of heart and spleen tissue as well as blood work for markers of cardiomyocyte death revealed that mice experienced higher viral burden, increased viral cytotoxicity and enhanced levels of infiltrating immune cells if their immunoproteasome function was inhibited before infection. This indicated a positive effect for sustained rather than impaired immunoproteasome function in this model for CVB3-myocarditis and prompted further inquiry into ONX 0914's inhibitory capacity

and efficacy on the level of protein expression of the immunoproteasomes subunits. Interestingly, in experiments where the immunoproteasome was inhibited after mice had already been infected with CVB3, we found no harmful effect of treatment with ONX 0914 compared to the vehicle in this mouse model, indicating that the immunoproteasomes key role during viral inflammation lies in the early stages of immune response and calling into question whether immunoproteasome-inhibition might enhance other pro-inflammatory compensating mechanisms.

1. Introduction

1.1 Myocarditis

1.1.1 Aetiology and epidemiology

(Peri)myocarditis, or inflammation of the heart muscle, is an inflammatory disease that may be caused by a number of different reasons. In its 2015 Global Burden of Disease study the Lancet reported a prevalence of 7,993,000 cases for cardiomyopathy and myocarditis worldwide (1). Additionally, there are mild, nearly asymptomatic as well as chronic courses of the disease, making an accurate overall estimate of occurrence nearly impossible. To aid in giving a more complete picture, it can be helpful to divide the causes of myocarditis into inflammation of infectious or non-infectious origin. About 50% of infectious myocarditis is thought to be caused by or post infection with cardiotropic viruses. In general, viral myocarditis is the most common non-ischemic cause of heart failure in the Western world (2). However, bacteria, fungal infection and some parasites can also lead to heart muscle inflammation in immunocompromised patients.

In non-infectious myocarditis, inflammation can be triggered by autoimmune processes such as in rheumatoid arthritis, vasculitis or other diseases that affect the body's connective tissues (3, 4). Additionally, hypersensitivity drug reactions, immunosuppressive medication and radiation of the mediastinum can initiate myocardial inflammation. Interestingly, cases of fulminant autoimmune myocarditis have been reported as a serious adverse reaction to treatment with immune checkpoint inhibitors (ICI), that are increasingly being used as novel cancer treatments (5). Cardiac pathology has also emerged as a rare but devastating complication of

treatment with proteasome inhibitors (6). Taken together, both viral and autoimmune mechanisms, sometimes sequentially, can cause and sustain myocarditis – they do so under the influence of a common downstream key immune effector, the Ubiquitin-Proteasome System.

1.1.2 Cardiac inflammatory processes

By whichever pathogen myocarditis is initiated, an acute and overwhelming inflammatory reaction including infiltration of immune cells into heart muscle tissue may result from all of the above-mentioned causes. Subsequently, experimental mouse models show not only disturbance of cardiac function and scarring of muscle tissue, termed cardiac remodeling, but also a systemic disequilibrium manifesting itself as a sepsis-like phenotype with high inflammatory markers, hypothermia, extensive weight loss and an appearance of generalized illness in affected animals (7). In humans, symptomatic patients may present with chest-pain, palpitations, arrhythmias and heart block, shortness of breath and pulmonary edema. Long-term damage of chronic myocarditis by smoldering myocardial inflammation includes dilated cardiomyopathy, heart failure and sudden cardiac death. The general notion is that both an immune cells' cross-reactivity to viral and myocardial structures as well as direct viral cytotoxicity result in a self-antigen immunoreaction, leading to and aggravating the inflammation in-situ. Fittingly, during the course of acute myocarditis, the development of anti-cardiac autoantibodies has been shown in mouse models (8).

Viral myocarditis is often caused by Coxsackie- or Parvovirus, but can also occur in patients infected with Influenzavirus, Coronavirus, Human Herpesvirus 6, Epstein-Barr-Virus and some other commonly recognized culprits. Here, research is mostly focused on extensively characterized experimental models, with the route and course of cardiac infection with cardiotropic Coxsackievirus B3 (CVB3) in mouse models among those especially well understood (9). CVB3 belongs to the Picornaviridae and is a single-stranded RNA virus. In experimental models using CVB3 susceptible strains such as A/J or NMRI mice, infection commonly leads to pancreatitis with destruction of exocrine function and to myocarditis (10). For myocarditis, direct viral cytotoxic effects are suggested by the detection of CVB3 RNA in murine heart muscle tissue during acute inflammation. Additionally, the induction of immune and autoimmune

mechanisms is responsible for cardiac inflammation in these animals and is seen as immune cell infiltration into the myocardium that can be characterized both histologically as well as by flow cytometric cell differentiation. Furthermore, a study using transgenic mice expressing CVB3-RNA at low-level to mimic persistent, non-infectious CVB3-infection in the heart demonstrated heart muscle fibrosis and cardiomyocyte degeneration as well as negative impact on cardiac function, showing that chronic CVB3 infection can trigger cardiac remodeling processes (11). In addition, ongoing viral myocarditis has been shown to act as a trigger for the development of cardiac autoimmunity. Typically, however, acute inflammation causes an immune response, which results in clearance of the infection with removal of affected cardiomyocytes and in consecutive restitution over time.

Regarding to the mouse models used, we and others have previously found that murine genetic background is of central relevance for development and outcome of CVB3-myocarditis (7, 12). Mice on an A/J and NMRI background are highly susceptible, but show vastly different phenotypes and reactions to treatment. C57BL/6 mice on the other hand, are a strain with low susceptibility and develop myocarditis to a much lesser degree.

1.2 Ubiquitin-Proteasome System and the Immunoproteasome

1.2.1 Ubiquitin-Proteasome System - function and functional changes

The Ubiquitin-Proteasome System (UPS) is well known for functioning as the cells "trash can", degrading misfolded and faulty as well as regulatory proteins to balance a cell’s proteostasis. On closer inspection, it has a number of other centrally important functions that are relevant to the above-described immune responses in myocarditis of any aetiology. It regulates cell-signaling, transcription, immune cell proliferation and, by processing intracellular pathogens and cleaving their peptides determines antigen presentation. Thus, the UPS plays a major role in modulation of the adaptive immune response (13).

Part of this highly sophisticated system is a large protein complex with a cylindrically stacked appearance, called the proteasome. In concert with ubiquitin, the key molecule which serves as a degradation signal by covalent attachment to the targeted protein,

the proteasome itself consists of a 20S core complex with internally active enzymatic subunits ß1, ß2 and ß5 that are organised into multi-subunit rings.
To mark a protein for degradation, it passes through multiple enzymatic steps, which are facilitated by numerous enzymes including ubiquitin-activating enzyme (E1), ubiquitin-conjugating enzyme (E2) and ubiquitin-protein ligase (E3)(14). Once successfully 'tagged', the protein is recognised by a 19S regulator associated with the 20S proteasome. Through peptide hydrolysis, ubiquitin is detached and the target protein is dismantled into peptides (15, 16) which can be loaded onto presenting molecules, the major histocompatibility complexes (MHC) I or II. They are then transported to and presented at an antigen presenting cell's (APC) surface, where interaction with $CD4^+$ T helper cells (via MHC II) or $CD8^+$ T cells (via MHC I) is needed to activate an immune response. Under certain conditions, such as inflammation or oxidative stress, cells may require a more rapid turnover of proteins, which otherwise collect into intracellular aggregates, disrupting cellular functions and have been shown to cause a number of different diseases (17-19). To manage this disruption and to exert its regulatory functions on the immune response, expression of the 20S proteasome is upregulated and additionally in some cells, a proteasome isoform – the immunoproteasome, as detailed below – is expressed (20).

1.2.2 Immunoproteasome - induction and role in inflammation

Pro-inflammatory cytokines and chemokines as well as some chemotoxins – simply put, anything that causes cellular stress – have been shown to induce the expression of a proteasome isoform called the immunoproteasome, harboured mainly in immune cells of hematopoetic origin. Subsequently, during inflammation, studies show a marked increase of this inducible isoform. In immune cells, the immunoproteasome represents the main proteolytic machinery with the standard version playing less of a role and here, baseline levels of immunoproteasome expression are high. In other cells, however, at baseline, the immunoproteasome is not typically expressed. In the inflamed heart, strong signals of immunoproteasome expression have been detected in conjunction with Interferon-signaling (21, 22). In other, more immunorelevant organs such as the spleen, high basal levels of this isoform are expressed even in the absence of pro-inflammatory triggers. Compared to the standard proteasome, the

immunoproteasome carries alternative enzymatic subunits that change its structural conformation and proteolytic activity. Corresponding to ß1, ß2 and ß5 in the standard proteasome, the isoform includes ß1i (LMP2), ß2i (MECL-1) and ß5i (LMP7) instead. Within it's built, the allocation of both ß1i and ß2i, and thereby its functionality, is dependent on the correct placement of ß5i. The immunoproteasome's adaptations under conditions of stress aid in maintaining a cells' protein homeostasis. They also significantly alter antigen generation by disparate cleaving of proteins for MHC-presentation, compared to the epitopes generated by its standard counterpart under baseline conditions. For example, studies comparing MHC I-related epitope generation in triple knock-out (ko) mice (meaning devoid of any immunoproteasome expression) and wildtype mice revealed that immunoproteasome function is necessary for this process, leaving ko mice with a strongly impaired and diminished repertoire of presented peptides (23).

1.2.3 Immunoproteasome inhibition

We and others have shown previously that while this multi-catalytic protein complex plays an important role in mounting a sufficient immune response, an overactive immunoproteasome can also have detrimental effects on an organism in regard to induction of an overwhelming inflammatory response, inducing a sepsis-like phenotype in affected mouse strains. Immunoproteasome inhibition has subsequently been shown to have a protective effect on the development of viral and autoimmune inflammatory diseases (7)(24-26). Yet, in the project presented here, we have also established that pharmaceutical inhibition of the immunoproteasome in NMRI mice during CVB3-myocarditis can lead to increase of virus-mediated tissue damage (12). In accordance, Mundt et al. have described that immunoproteasome inhibition does not aid in survival of allogenic skin-grafts and the pathogenic course of Candida albicans infection is another condition that cannot be ameliorated in this way, thus supporting the notion that not all immunoproteasome inhibition has a beneficial immunoregulatory effect (27, 28). Essentially, specific inhibition of the immunoproteasome has emerged as a double-edged sword.

Proteasome inhibition, affecting all isoforms, is a known treatment option for multiple myeloma. Cancer cells, with their rapid turnover rates rely on the UPS' function more heavily than most other tissues, making the proteasome a sensible target for stunting

their growth and ability to divide. Naturally, side effects most often affect organ systems that depend on regular turnover as well, with some of the most common adverse events to treatment with proteasome inhibitors being neutropenia and anemia as well as diarrhea and peripheral neuropathy (29). Both to mitigate these often dose-limiting toxic effects as well as to research a more specific blockade of the proteasomes' processes and role in driving and sustaining inflammation and cellular homeostasis, immunoproteasome inhibitors have been a focus of experimental work for many years. This is mainly connected to the discovery that at baseline, immune cells and immunorelevant organs express high levels of the immunoproteasome and low levels of standard proteasome while for most other cells, the opposite is true.

Experimental setups to this effect are designed to disrupt immunoproteasome function more selectively, and thereby mitigate overwhelming inflammation by uncontrolled immune cell activity as well as smoldering inflammatory processes such as in chronic disease and malignancy. In order to understand the ramifications of immunoproteasome inhibition *in vitro* and *in vivo*, different models have been developed. Since successful incorporation of the immunoproteasomes active subunits ß1i/LMP2 and ß2i/MECL-1 is dependent on ß5i/LMP7 placement, targeting this subunit with specific inhibitors is a logical place to start. Apart from knock-out mice that may either be devoid of LMP7, LMP7 and LMP2 or all three subunits (triple knock-out), immunoproteasome inhibitors, of which ONX 0914 is best characterized, are widely used to that effect.

1.3 Relevance

1.3.1 Questions raised in this project

In work previously done by our group, we were able to demonstrate that acute viral myocarditis in A/J mice, who are highly susceptible to CVB3-induced cardiac pathology and experience significant viral burden, can be mitigated to a considerable degree by inhibition of the immunoproteasome either by genetic knock-out or by pharmaceutical targeting (7). Mice that were treated with the epoxyketone compound ONX 0914 before infection with CVB3 had better overall outcome, including survival when compared to their placebo-treated controls. This led us to believe that disrupting immunoproteasome function could potentially even have a protective effect on long-

term sequelae of ongoing enterovirus myocarditis. Since A/J mice became so severely ill when exposed to the virus, we aimed to transfer our experimental protocol to a different mouse strain, outbred NMRI mice, that have previously been shown to develop CVB3-induced chronic myocarditis while experiencing relatively few concerning symptoms such as excessive weight loss, hypothermia and lethargy. Additionally, treating mice with the compound before inoculation with the virus raised the question of whether immunoproteasome inhibition could also have a therapeutic effect on development of CVB3-myocarditis if initiated after induction of the inflammatory response. Our question was if by successfully treating the acute inflammation at a symptomatic state, could we then prevent, to some extent, cardiac remodeling and heart failure over time?

As severe side effects of proteasome inhibitors were already known and events of autoimmune-myocarditis in patients receiving ICI therapy started to emerge, we, together with our cooperation partners at the University of Heidelberg decided to then broaden our scope to another project (30, 31). Parallel to our work with the virus but nevertheless intertwined by the role of UPS in inflammation, we sought to elucidate the immunological effects of immunoproteasome ablation and blockade in a model for autoimmune-related myocarditis. Additionally, virus-mediated heart disease can serve as a trigger for cardio-directed autoimmunity, as shown by the appearance of TnI-autoantibodies in chronic viral myocarditis, which further affirmed our scientific interest in this possible connection.
Since the UPS in all its isoform variants has demonstrated such wide-ranging and significant functions for modulating immune responses, uncovering more about the underlying mechanisms as well as further detailing its role in both an infectious and non-infectious context will be crucial to finding new targets that will enable us and others to take our research from bench to bedside. As this project, however, was not the initial focus of the dissertation and all experiments were carried out in cooperation, its results and implications will not be discussed as results of this work.

2. Methods

Mouse model

ONX 0914 is an epoxyketone-based compound and irreversible inhibitor of the immunoproteasome. It binds to the functionally important immunoproteasome subunit ß5i/LMP7, thereby preventing its binding to a polypeptide for hydrolytic purposes, essentially rendering the immunoproteasome void of its function.
We purchased the compound from Cayman Chemicals. For experimental purposes, it was dissolved to a concentration of 1mg/ml of Captisol and sodium citrate at a pH of 3.5. A solution of Captisol at 1mg/ml with sodium citrate at pH 3.5 without the addition of ONX 0914 was used as the vehicle. Aliquots of both ONX 0914 and the vehicle were stored at -20°C. It was injected subcutaneously as per the manufacturer's instructions.

The model used for viral myocarditis by CVB3 infection of mice is well established in our group. For this project, however, we purchased male outbred NMRI mice in place of the A/J strain or C57BL/6 strain utilized before. After an adaptation period of 1 week at the animal housing facility at Charité University Medical Center in Berlin, mice were injected with a cardiotropic CVB3 strain (31-1-93) that has been used before and is well established inducing viral myocarditis specifically in this mouse strain (14, 45). Virus inoculation was performed intraperitoneally on day 0 of each experiment and mice were closely monitored throughout all experiments.
There were two main experimental schedules, one requiring injection with the immunoproteasome inhibitor ONX 0914 or the vehicle from one day prior to viral infection, which was defined as day 0 in all experiments and one where mice were treated from day 3. In either case, ONX 0914 or the vehicle were administered daily until day 8. To allow for the extended time it takes to develop chronic myocarditis in sequence to the acute infection, mice in that group continued treatment with the inhibitor or placebo three times per week until day 28. Additionally, on day 0 and the final day of each experiment, transthoracic echocardiography was performed to assess cardiac function before and after infection and treatment. Mice were put to sleep using isoflurane in an O_2/gas mixture and closely monitored for both body temperature and changes in ECG. Echocardiography measurements were then performed by an experienced technician from the animal research facility at Max-Delbrück Centre in Berlin who was blinded to all treatment allocations on a VisualSonics Vevo770 or

Vevo3100 High-Frequency imaging system using scan head CRMV-707B at 15-45Hz. We received their raw datasets, which were then statistically analyzed.
On the final day of all experiments, organs were collected and frozen for the following analyses. Blood was centrifuged to collect serum for profiling of cytokines/chemokines as well as levels of Troponin T (another highly cardiospecific protein).

Flow cytometry

We aimed to quantify immune cell infiltration into heart muscle tissue as well as T cell distribution and activation at different time points during etiologically different courses of myocarditis.
Murine hearts were washed with PBS and a piece was cut, weighed and stored in a buffer containing RPMI 1640 with 2% FBS, 1% Pen/Strep and 30mM HEPES. Digestion of tissue to extract cells was accomplished with Collagenase by Worthington Biochemical Corporation and DNAse I. 10mM of EDTA was added and cells were strained through 70µm of mesh to generate a single-cell suspension. Erythrocyte lysis was performed with a lysis buffer. Fc-receptor blocking agent was added to a volume corresponding to 20mg of tissue. For exact antibodies used for staining as well as gating strategies, please refer to the methods and supplemental sections of our publications (14, 22). After several more washing steps, stained cells were incubated with Fixable Viability Dye and then fixed in 2% formaldehyde in PBS. 123count eBeads were added to later be able to quantify cell numbers. We used a BD FACSymphony flow cytometer, analyzing data with FlowJoV10 software.

Western blot and protein expression

In order to understand the impact of ONX 0914 on expression of the immunoproteasome and standard proteasome subunits during myocarditis, visualization and quantification of protein expression was another essential step in our experiments. This was achieved by standard western blotting for all catalytic subunits. Prior to application onto the gel, tissue samples from both heart and spleen were homogenized in lysis buffer. To determine protein concentrations and volumes to be added, Bradford assay was performed. After dilution, samples were applied, run and tank blotting was performed. Primary and secondary antibodies used for staining are

available upon request. Blots were detected on an Odyssey CLx imager by Li-Cor Bioscience. In spleen tissue especially, high total number of proteins accounted for poor comparability due to high background signals, distorting both densitometric analysis as well as control for equal loading. To combat this issue, a total protein stain was used for normalization and protein bands were quantified by ImageStudio Light 5.2 software (Li-Cor Bioscience). Heart tissue samples were normalized to ß-actin.

Quantitative PCR (qPCR)

For detection of viral RNA at different time points, we performed RNA isolation, cDNA synthesis and qPCR using CVB3 probes normalized to mHPRT as a housekeeping control. RNA was first isolated from heart and spleen tissue separately using Trizol Reagent and samples were then treated with DnaseI. For cDNA synthesis we used random hexamer primers and MLV-reverse transcriptase. qPCR was performed on a StepOnePlus real time PCR system with TaqMan Fast Universal PCR Master Mix and primers/probes from TaqMan gene expression assays.

Histology and quantification of infectious particles

To look for immune cell infiltration and markers of acute and chronic inflammatory processes, heart sections were fixed in 4% formaldehyde and sliced 5µm thick before staining with hematoxylin/eosin and Masson's trichrome. This part of the analysis was done by Prof. Klingel's team at the University of Tuebingen's Institute of Cardiopathology. Essentially, thirty visual fields at a magnification of x160 are analyzed manually for myocardial damage including cardiomyocyte necrosis, infiltration with immune cells and scarring. The area of damaged myocardium in relation to the total area is then calculated to a myocarditis score ranging from 1 (very mild) to 4 (severe) (45).

Titers of infectious virus in plaque forming units (pfu) was calculated with the help of standard plaque assay on HeLa cells, cultivated in monolayer and were performed in duplicates. 10-fold titrations of homogenized heart sections from infected animals were incubated on the cells and supernatant was then discarded before agar overlays were applied. After incubation (48h), MTT-stain revealed number of plaques which were

counted to determine concentration of active infectious particles at different time points.

Statistical analysis

For statistical analysis, GraphPad Prism 7.0 Software was used. Some data was transformed logarithmically before plotting and analyzing and this is indicated in that data. Normal distribution was determined using D'Agostino Pearsons normality test. Normally distributed data was analyzed by unpaired or paired t-test while non-normally distributed data was analyzed using Wilcoxon-signed rank test or Mann-Whitney test. Repeated measurements such as time points or treatment group comparisons were done using two-way ANOVA with Sidak's multiple comparison where indicated. Data is displayed as mean ±SEM unless indicated otherwise.

3. Results

NMRI mice develop CVB3-myocarditis

The aim of this project was to gain further insight into the effects of specific immunoproteasome inhibition in models of CVB3-induced cardiac inflammatory disease. Specifically, the therapeutic capacity of immunoproteasome inhibition and modulation of immune response during the acute and chronic phase of inflammation

were of interest. Experimental schedules were developed for both acute and chronic

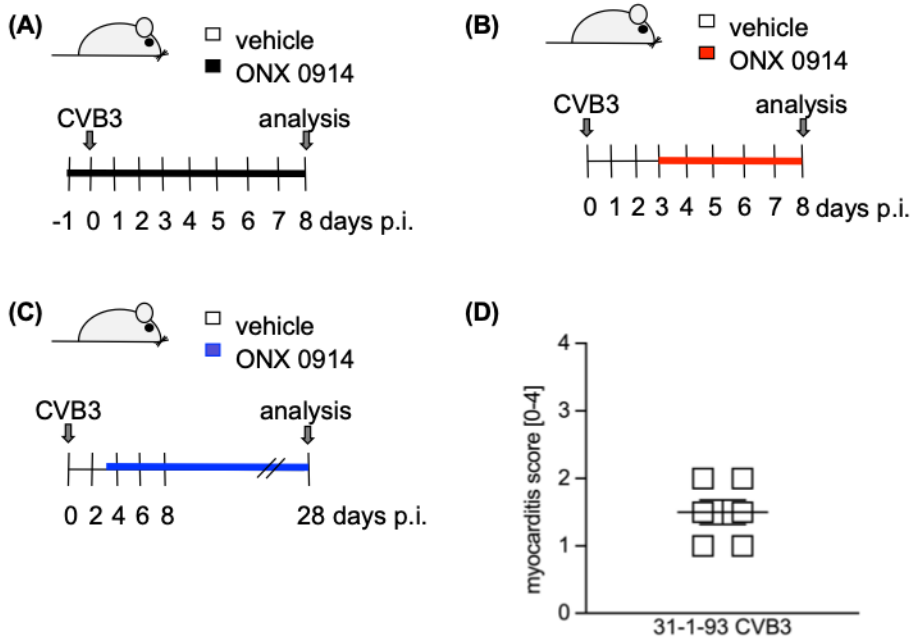

figure 1. experimental schedules for viral myocarditis mouse models
(A) experimental schedule for acute viral myocarditis using a prophylactic (application of ONX 0914 or the vehicle from day -1) or (B) therapeutic approach (application of ONX 0914 or the vehicle from day 3). (C) experimental schedule for chronic viral myocarditis, starting treatment with ONX 0914 or the vehicle from day 3. (D) histological myocarditis score comprising both inflammation and fibrosis in heart tissue of NMRI mice 28 days after inoculation with CVB3, scoring from (1) very mild to (4) severe myocarditis.

phase mouse models and are shown in *figure 1 A-C*.

In establishing the mouse model and before proceeding with our experiments, we inoculated NMRI mice with CVB3 on day 0, confirming histologically on day 28 post-infection that we could experimentally establish myocardial inflammation to a significant degree in this breed *(figure 1D).*

As expected for this mouse strain, NMRI mice proved clinically more robust in their phenotype and in contrast to our previously reported results in A/J mice, no comparable decline of general health by virus inoculation was noted in this breed. Accordingly, in the following experiments, NMRI mice largely maintained their weights and cardiac function as measured by echocardiography throughout the course of CVB3-myocarditis, the presence of which was confirmed histologically.

Consequentially, we showed that NMRI mice inoculated with the dose of CVB3 virus given in these experiments did develop myocardial inflammation, giving way to further investigation using this mouse model.

Treatment with ONX 0914 has no protective effect on development of chronic myocarditis in NMRI mice

In a first investigative approach, NMRI mice were randomized to two groups, receiving either the vehicle or ONX 0914 as a treatment. The question posed in this experiment was if ONX 0914, given to NMRI mice, could alter the course of the infection and have a protective effect on cardiac tissue. Echocardiographic measurements were analyzed

parameter	vehicle		ONX 0914	
	baseline	day 28	baseline	day 28
Heart rate [bpm]	417 ± 18	440 ± 18	440 ± 18	426 ± 14
Trace EF [%]	46 ± 2.5	48.1 ± 2.9	43.6 ± 2.6	42.7 ± 2
Cardiac output [mL/min]	13.6 ± 1	14.6 ± 1	14.3 ± 1.1	14 ± 0.8
Stroke volume [µL]	32.4 ± 1.8	32.7 ± 1.5	32 ± 1.9	33 ± 1.8

table 1. effect of ONX 0914 treatment on cardiac function in NMRI mice with chronic CVB3-myocarditis
Echocardiography was performed at baseline (day 0) and on day 28 in mice inoculated with CVB3 and treated with either ONX 0914 or the vehicle for 28 days. Heart rate (bpm), Trace ejection fraction (EF, in %), Cardiac output (mL/min) and Stroke volume (µL) are among the key parameters to determine changes in cardiac function.
table 1 was adapted from Neumaier et al., Cells 2020 DOI:10.3390/cells9051093

to compare a possible effect on cardiac function in both treatment groups *(table 1).* However, no significant effect by ONX 0914 treatment was detected in these studies. We found that cardiac function as indicated by left ventricular ejection fraction and stroke volume were comparable to baseline measurements. Additionally, tissue samples from the heart of mice in both treatment groups were analyzed for residual CVB3-genome using qPCR to determine any persistent viral activity at this point in infection. In both groups, no such viral persistence could be detected with both groups showing histological signs of inflammatory tissue damage in the heart but lacking any

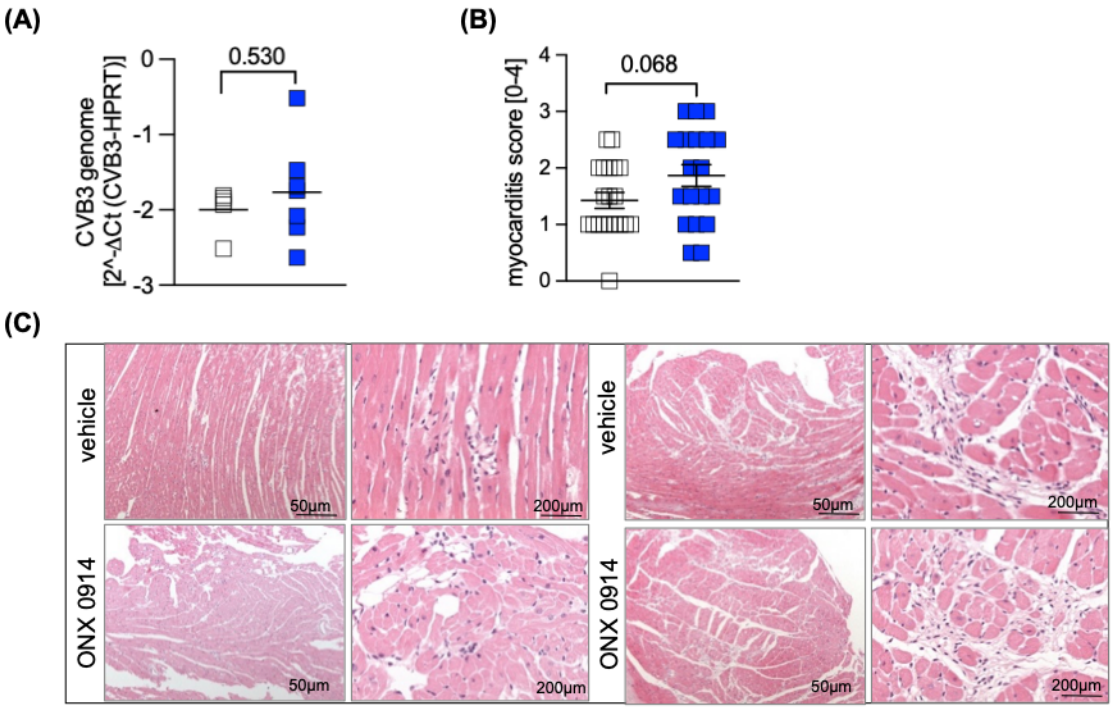

figure 2. Effect of ONX 0914 treatment on the development of chronic viral myocarditis in NMRI mice.
(A) mRNA expression of CVB3 genome for NMRI mice treated with either ONX 0914 or the vehicle on day 28 post-infection. Treatment was initiated on day 3 and mice received injections daily until day 8. Thereafter, treatment continued every other day. (B) histological myocarditis score comprised of both inflammation and fibrosis in heart sections from CVB3-infected NMRI mice in either the vehicle or ONX 0914 group. (C) microscopic images of heart sections from mice in both groups, showing immune cell infiltration on day 28, magnified at 50µm and 200µm per cm.
figure 2 was adapted from Neumaier et al., Cells 2020 DOI:10.3390/cells9051093

indication of ongoing viral replication *(figure 2)*. While this experiment clearly demonstrated that there is no significant protective effect of ONX 0914 treatment on the hearts of NMRI mice during chronic CVB3 infection, if treatment is initiated on day 3 post-infection, we did notice a tendency towards higher histological myocarditis scores in ONX 0914 treated animals.

A dysfunctional immunoproteasome during acute CVB3-myocarditis has potentially harmful effect on NMRI mice

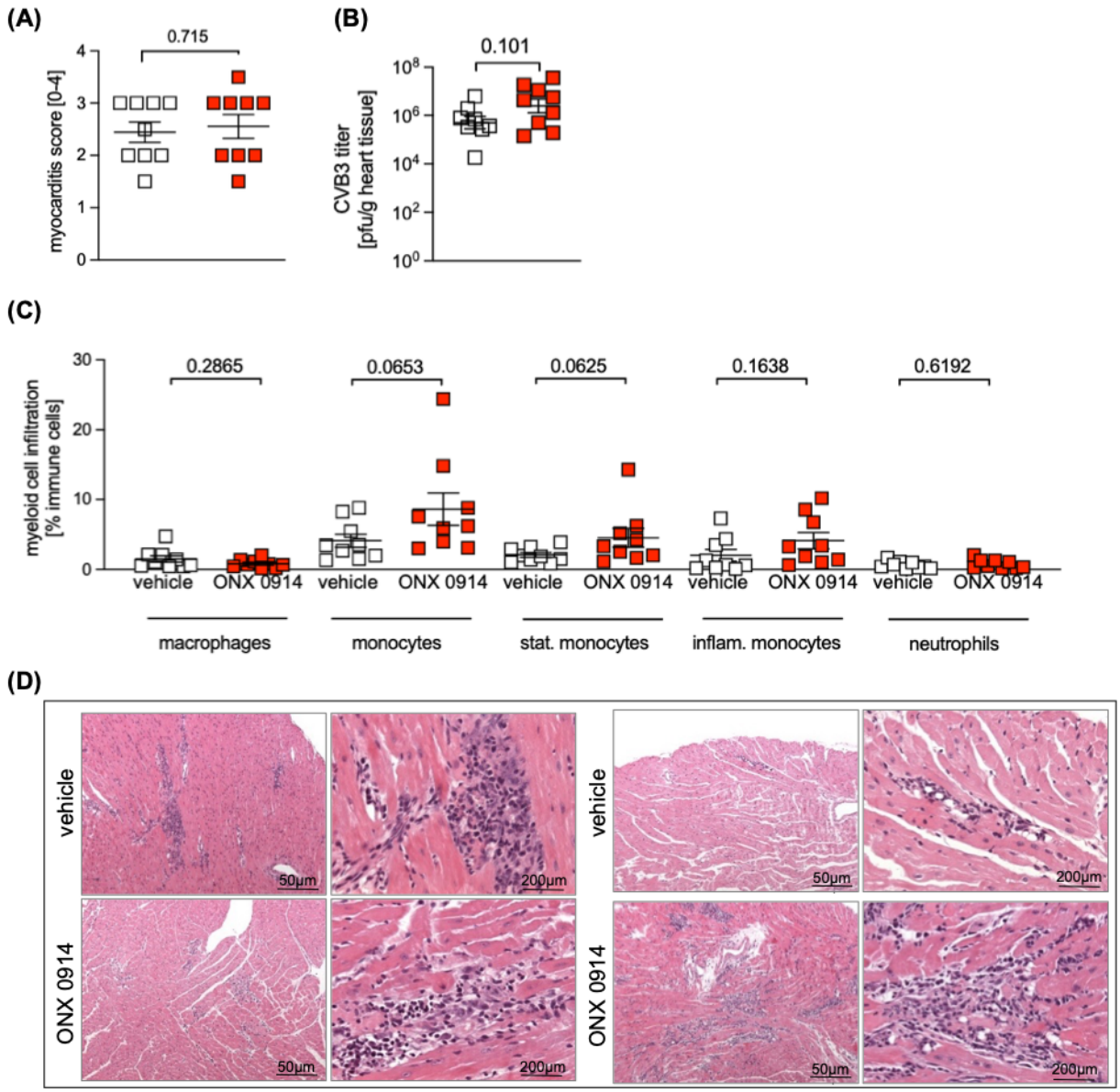

figure 3. Effect of ONX 0914 treatment on acute viral myocarditis in NMRI mice.
Mice in both treatment groups were inoculated with CVB3 on day 0. From day 3 to day 8, they were treated with ONX 0914 or the placebo daily. Tissue was analyzed thereafter.
(A) myocarditis score as determined by histological scoring of heart sections from NMRI mice in both treatment groups for inflammation and fibrosis on day 8. (B) mRNA expression of CVB3 in both groups on day 8. (C) FACS analysis of numbers of infiltrating immune cells into heart tissue of mice from both treatment groups (in %) (D) histological heart sections from both treatment groups stained for immune cell infiltration (tissue samples collected on day 8).
figure 3 was adapted from Neumaier et al., Cells 2020 DOI:10.3390/cells9051093

Leading on from the previous section, in a next step, we wondered whether effects of ONX 0914 treatment could be measured at an earlier stage during the inflammatory process, such as had been shown for other mouse strains in experiments published by our group previously (7, 32). We therefore aimed to test our therapeutic approach during the acute phase of myocarditis. Both treatment groups received daily injections of either ONX 0914 or the vehicle from day 3 until day 8 after virus inoculation on day 0. After analysis, no effects were noted for histological changes in heart tissue between treatment groups with both treatment groups showing inflammatory tissue changes to

a comparable degree (*figure 3A+D)*. Surprisingly, we did see a non-significant tendency towards higher numbers of plaque-forming CVB3 units per gram of heart tissue, indicating higher viral load, in the animals treated with ONX 0914 (*figure 3B)* in these experiments as well. As these results were reminiscent of the protective effect of keeping the immunoproteasome intact during infection that has been shown for a different mouse strain, C57BL/6 mice, we wondered whether NMRIs 'immune system might also benefit from undisturbed immunoproteasome function when fighting CVB3-myocarditis (7, 32). Additionally, we identified heart infiltrating immune cells via flow cytometric analysis in both groups, revealing that mice receiving ONX 0914 had higher numbers of infiltrating monocytes, of which a significantly higher number were classed as inflammatory monocytes compared to vehicle-treated animals (*figure 3C)*. Other cell types of the same myeloid origin such as neutrophils and macrophages, in turn were balanced in their numbers between treatment groups. However, as these effects were not yet entirely clear, we aimed to define and characterize further, how inhibition of the immunoproteasome influences the course of Coxsackievirus myocarditis in this strain.

preemptive ONX 0914 treatment causes enhanced inflammatory response in NMRI mice

To answer the questions posed after our experiments using ONX 0914 in a therapeutic approach, we diverted back to an original experimental schedule previously used for experiments of acute myocarditis in A/J mice. NMRI mice were randomized to a vehicle-receiving and an ONX 0914-receiving group and treatment was started on day -1, one day before CVB3-inoculation. Treatment was continued daily until day 8. Here, a much clearer picture emerged. While both treatment groups developed viral myocarditis, mice treated with ONX 0914 showed significantly enhanced inflammatory response *(figure 4)*. These animals had a tendency towards higher histological myocarditis scores, showed significantly higher numbers of TroponinT, used as a marker for cardiac tissue damage, and correspondingly exhibited higher myocardial viral load, when compared to the animals receiving the vehicle. Flow cytometric analysis revealed a significantly larger burst in infiltrating inflammatory monocytes for the ONX 0914-group as well. As all of these results are mere downstream characteristics for effects of upstream proinflammatory cytokines and chemokines, we

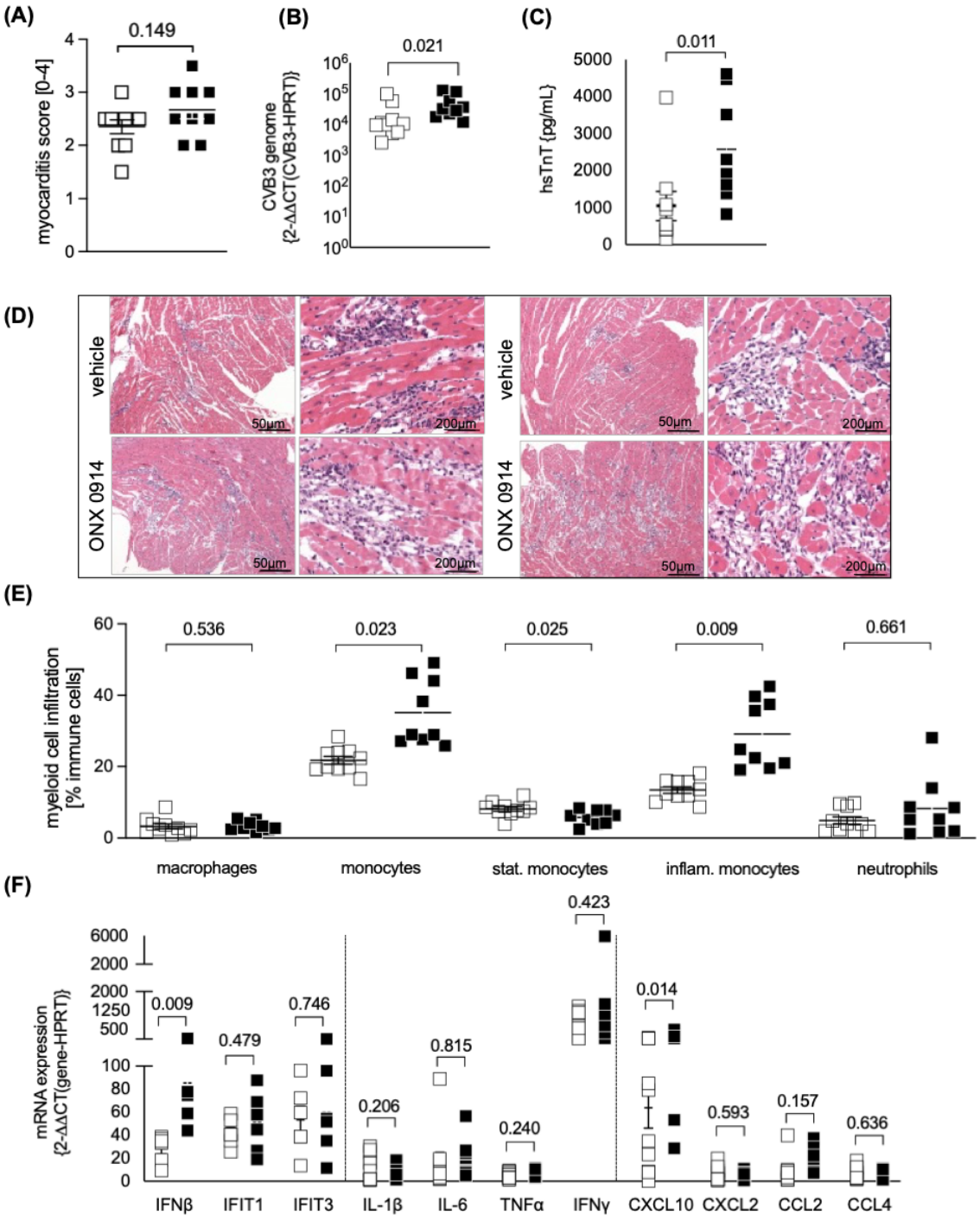

figure 4. Effect of preemptive immunoproteasome blockade on acute viral myocarditis in NMRI mice.
Mice in both treatment groups were inoculated with CVB3 on day 0. Treatment began on day -1 and the vehicle or ONX 0914 were applied daily until day 8.
(A) myocarditis score as determined by histological scoring of heart sections from NMRI mice in both treatment groups for inflammation and fibrosis on day 8. (B) mRNA expression of CVB3 genome in heart tissue of CVB3-infected NMRI mice on day 8 treated with ONX 0914 or the vehicle from day -1 (C) high-sensitive TroponinT levels in heart tissue of CVB3-infected NMRI mice on day 8 treated with ONX 0914 or the vehicle from day -1 (D) histological heart sections from NMRI mice with acute viral myocarditis, treated with the vehicle or ONX 0914. (E) FACS analysis of numbers of infiltrating immune cells into heart tissue of mice from both treatment groups (in %) (F) mRNA expression of different proinflammatory cytokines and chemokines on day 8 in CVB3-infected NMRI mice treated with ONX 0914 or the vehicle from day -1.
figure 4 was adapted from Neumaier et al., Cells 2020 DOI:10.3390/cells9051093

analyzed heart tissue from both treatment groups for mRNA expression of different

common cytokine/chemokine triggers that aid in facilitating an inflammatory response. Interestingly, we found that while IFNβ was expressed significantly more in ONX 0914-treated mice, the thereby inducible proteins IFIT1 and 3 were not. Other cytokines and chemokines such as TNFα, IL-1β, IL-6 and IFNγ as well as CCL2 and CCL4 were similarly upregulated in both treatment groups. CXCL10, however, a chemoattractant induced by IFNγ and secreted by monocytes among others, was expressed significantly more in the group receiving ONX 0914. On a functional level, echocardiography revealed reduced left ventricular ejection fraction in the ONX 0914 group *(table 2)*. However, both groups had reduced cardiac output on day 8 when

parameter	**vehicle**		**ONX 0914**	
	baseline	day 8	baseline	day 8
Heart rate [bpm]	427 ± 16 §	393 ± 16	500 ± 13 §,*	405 ± 23 *
Trace EF [%]	50.7 ± 1.7	48.4 ± 2.6	57.4 ± 2.3 *	49.1 ± 3.2 *
Cardiac output [mL/min]	14.4 ± 1.2 §,*	10.0 ± 0.9 *	18.6 ± 1.2 §,*	12.1 ± 1.3 *
Stroke volume [µL]	33.6 ± 2.1 *	25.2 ± 1.4 *	37.3 ± 2.4 *	29.6 ± 2.3 *

table 2. Effect of preemptive immunoproteasome blockade on cardiac function in NMRI mice with acute CVB3-myocarditis
Echocardiography was performed at baseline (day 0) and on day 8 in mice inoculated with CVB3 and treated with either ONX 0914 or the vehicle from day -1. Heart rate (bpm), Trace ejection fraction (EF, in %), Cardiac output (mL/min) and Stroke volume (µL) are among the key parameters to determine changes in cardiac function. §: significant difference between treatment groups at baseline or day 8; *: significant difference comparing baseline to day 8 within a treatment group.
table 2 was adapted from Neumaier et al., Cells 2020 DOI:10.3390/cells9051093

compared to their respective baseline measurements.

ONX 0914 unselectively inhibits standard proteasome subunit β5 in NMRI mice

After the unexpected results obtained in regard to an enhanced inflammatory response in the hearts of ONX 0914-treated NMRI mice, we started looking at the effects that inhibition of the immunoproteasome had on the enzymatically-active subunits within this proteolytic complex *(figure 5 adapted from (12) figures 4 and 5)*. mRNA expression levels of both the standard and immunoproteasome subunits were measured, followed by westerns blotting for the same subunits. This allowed a look at how gene expression

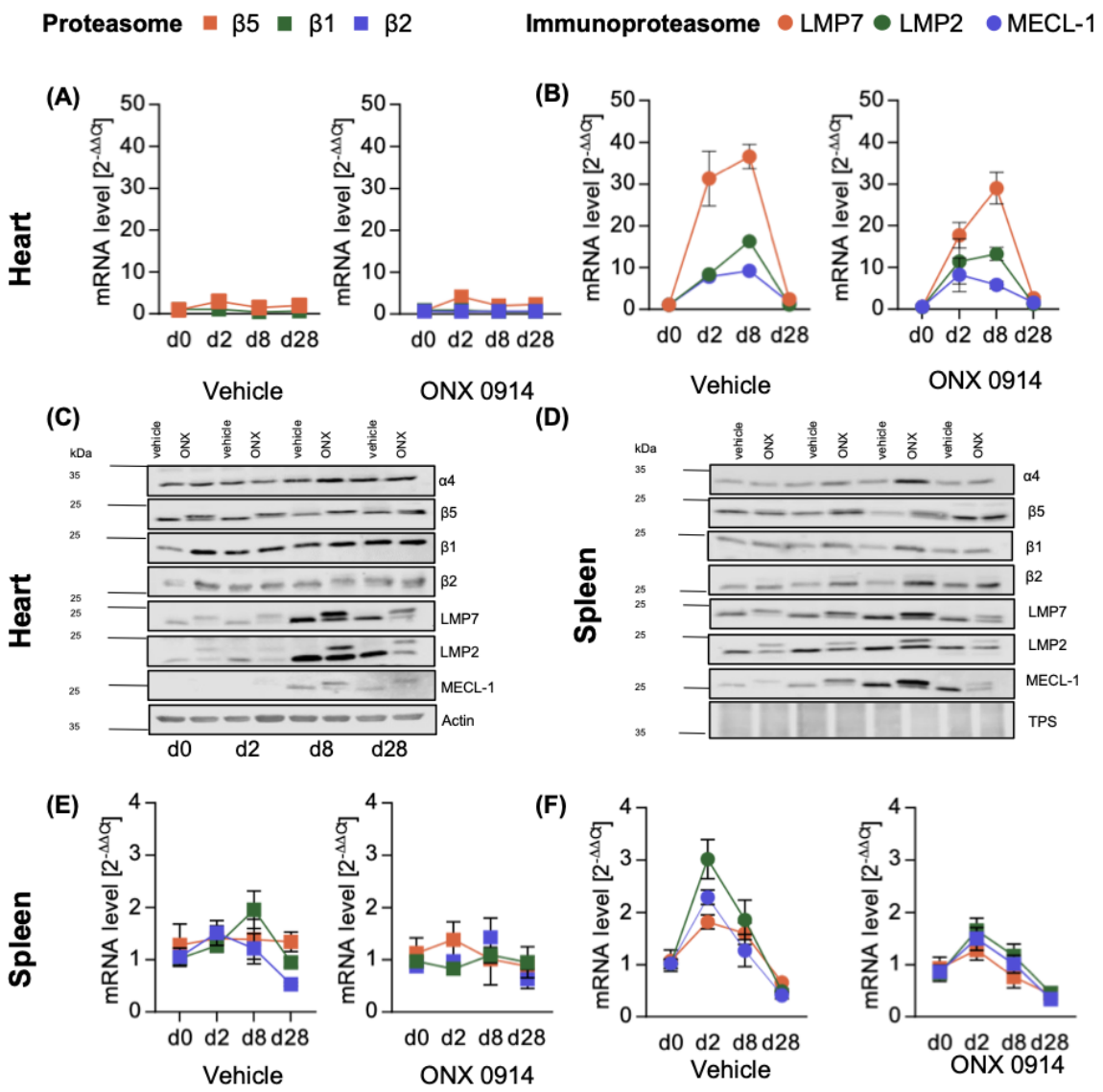

figure 5. mRNA and protein expression of standard and immunoproteasome subunits during CVB3-myocarditis in NMRI mice.
(A) mRNA expression of standard proteasome subunits in heart tissue of NMRI mice on days 0, 2, 8 and 28 during CVB3-myocarditis for animals treated with either ONX 0914 or the vehicle. (B) mRNA expression of immunoproteasome subunits in heart tissue of NMRI mice receiving either ONX 0914 or the vehicle on days 0, 2, 8 and 28 post infection. (C) western blots of both standard and immunoproteasome subunits with actin as a loading control for heart tissue of NMRI mice receiving ONX 0914 or the vehicle on days 0, 2, 8 and 28 post infection. Binding of ONX 0914 is signified by band shift towards a higher molecular mass. (D) western blots of both standard and immunoproteasome subunits with total protein stain (TPS) as a loading control for spleen tissue of NMRI mice receiving ONX 0914 or the vehicle on days 0, 2, 8 and 28 post infection. (E) mRNA expression of standard proteasome subunits in spleen tissue of NMRI mice on days 0, 2, 8 and 28 during CVB3-myocarditis for animals treated with either ONX 0914 or the vehicle. (F) mRNA expression of immunoproteasome subunits in spleen tissue of NMRI mice receiving either ONX 0914 or the vehicle on days 0, 2, 8 and 28 post infection.
figure 5 was adapted from Neumaier et al., Cells 2020 DOI:10.3390/cells9051093

might translate to protein expression in the context of immunoproteasome inhibition by ONX 0914. Here, our hypothesis was that ONX 0914 might show different inhibitory capacity for tissues with low baseline-levels of immunoproteasome such as the heart when compared to immunoproteasome-abundant organs like the spleen. Accordingly,

representative samples of both heart and spleen tissue were analyzed for standard proteasome subunits β5, β1 and β2 as well as immunoproteasome subunits LMP7, LMP2 and MECL-1, respectively. To give a more complete picture of the course of infection, we performed temporal subunit profiling using samples from day 0, day 2, day 8 and day 28 to compare treatment groups. mRNA expression results were randomized to standard housekeeping control mHPRT and western blot results were quantified by normalization to a total protein stain.

In splenic tissue, mice treated with the vehicle exhibited increased expression of immunoproteasome subunits on days 2 and 8 during acute infection, while levels returned to baseline on day 28. In mice with a dysfunctional immunoproteasome due to ONX 0914 treatment, subunit mRNA expression in the spleen did also generally increase during acute inflammation, albeit to a much lesser degree.

In the heart, mRNA expression of the immunoproteasome subunits LMP7, LMP2 and MECL-1 was markedly increased in both groups, which supports the observation of enhanced cardiac inflammatory response during acute myocarditis.

We found that, for all catalytic standard proteasome subunits, regardless of treatment group and throughout the course of infection, expression profiles remained largely the same in both the heart and spleen. However, when regarding to their respective protein expression levels, as determined by western blot, we found indications of a loss of efficacy for ONX 0914 over time. Binding of ONX 0914 to a subunit is indicated by a band shift on the western blot, corresponding to its higher molecular weight as opposed to when it migrates the gel without the addition of ONX 0914. Interestingly, in the hearts of NMRI mice treated with ONX 0914, the standard proteasome subunit β5 also appeared shifted by binding of the inhibitor on day 8, while the protein signal for subunit binding of LMP7 and LMP2 decreased proportionally.

Overall, we found that in the heart, where the immunoproteasome is induced and baseline levels are low, ONX 0914 shows modified inhibitory selectivity, targeting also the standard proteasome subunit β5, affecting the formation of this proteolytic core complex. In tissue where the immunoproteasome is naturally abundant, like the secondary lymphatic splenic tissue, ONX 0914 selectively inhibits the immunoproteasome but loses its efficacy over time.

4. Discussion

4.1 summary of results

This project served as a direct continuation of work previously done by our group involving CVB3-induced viral myocarditis in A/J mice that was successfully shown to be mitigated by application of an immunoproteasome inhibitor (ONX 0914) before inoculation with the virus. Additionally, in that publication, we also presented data showing that immunoproteasome ablation by LMP7 knock-out led to improved survival rates and protected A/J mice from severe viral myocarditis by Coxsackievirus B3 infection (7). Here, we asked whether a different mouse strain, NMRI mice, would also be protected from myocardial infection by application of ONX 0914. Additionally, we aimed to use ONX 0914 as a treatment after inoculation with CVB3, investigating if immunoproteasome inhibition in the context of an established immune reaction to CVB3 would result in a milder or even subdued immune response and alter the course of myocarditis. Leading on from our experimental approaches to better characterize acute CVB3-myocarditis, we also asked if pharmaceutical immunoproteasome inhibition in NMRI mice would impact the development of chronic myocarditis as a sequel to acute viral infection.

Unexpectedly, our results showed that while NMRI mice did develop acute viral myocarditis, subsequent application of the immunoproteasome inhibitor ONX 0914 did not lead to mitigated inflammatory response after 28 days nor did it serve to positively impact cardiac function over time as demonstrated by echocardiographic measurements. Instead, we observed a slight, non-significant tendency towards higher histological myocarditis scores. This observation did alter our original experimental plan regarding to a more thorough investigation into the effects of ONX 0914 on NMRI mice in this viral inflammatory context.

Subsequently, we decided to measure the effects of ONX 0914 on cardiac inflammatory disease during a more acute viral stage, after 8 days. Here, results showed that mice with a dysfunctional immunoproteasome had a tendency toward higher viral load in heart tissue as demonstrated by higher numbers of plaque-forming units of CVB3 per gram heart tissue. These animals also showed an increased number of infiltrating monocytes, differentiated by FACS analysis of heart tissue, however those numbers were not significant.

To further accentuate the effects of immunoproteasome inhibition in this context, mice received ONX 0914 before inoculation with CVB3. As a result, we found significantly heightened inflammatory response with higher viral load in the heart but sustained virus control in other tissues (spleen, pancreas), as well as higher levels of Troponin T, higher histological myocarditis scorings and reduced left ventricular ejection fraction in mice receiving ONX 0914.

Because of these results, we then asked which upstream pro-inflammatory cytokines and chemokines might be upregulated to explain our observed downstream effects. Results from mRNA expression analysis by qPCR from heart muscle tissue revealed a higher expression of IFNβ and CXCL10 in ONX 0914-treated animals. Western blot analysis of protein expression and qPCR for mRNA expression of immunoproteasome subunits as well as enzymatically active subunits of the ONX 0914-effect exempt standard proteasome subsequently revealed reduced selectivity for immunoproteasome subunit LMP7 and showed that ONX 0914 loses its efficacy over time, inhibiting standard proteasome subunit β5 as well. Accordingly, the use of ONX 0914 in NMRI mice for CVB3-induced myocarditis in both an acute and chronic inflammatory context, did not show any protective effect and rather led to an enhanced immune response, while animals with an intact immunoproteasome function showed sustained virus control, making a functional immunoproteasome the favorable state in this particular inflammatory context.

4.2 interpretation of results

Immunoproteasome inhibition by use of ONX 0914 has been a topic of investigation in our group as well as some other well published research groups for several years. Previously, in a study published in 2018, we shared data showing that for C57BL/6 (B6) mice, application of ONX 0914 before virus inoculation led to higher histological inflammation scores and increased viral load when compared to vehicle-treated littermate controls (7). A similar ONX 0914-mediated inflammatory exacerbation in B6 mice was shown for fungal infection with Candida albicans (27). Both studies suggest an effect on innate immunity through application of ONX 0914 that could be mediated by IFN response. However, as reported above, we did not find impaired, but rather enhanced IFN levels in NMRI mice who demonstrated higher viral load. However, it is possible that direct virus-host cell interaction plays a role in this observation, as

inhibition of the immunoproteasome could influence intracellular degradation of viral proteins and thereby stabilize virus replication to reflect higher pathogen burden. A similar effect has been extensively reviewed in work published by Kumar et al. only last year (33).

Even though generally results shown here for NMRI mice are partly reminiscent of findings for B6 mice, in the above-mentioned publication, for A/J mice, a mouse strain with high susceptibility to virus-induced myocarditis, an entirely different picture emerged. This breed could be protected from severe illness and survival dramatically improved in mice receiving ONX 0914, which was reflected in significantly reduced numbers of immune cell infiltrates found in heart muscle tissue 8 days after virus inoculation (7). Conclusively, in that study, we suggested that the severe pathology observed in mice with an intact immunoproteasome function could be attributed to an overpowering cytokine release and inflammatory reaction, which leads to a sepsis-like phenotype in A/J mice with CVB3-myocarditis. As NMRI mice, in contrast to B6 mice, are also known to be a susceptible breed in regards to CVB3-myocarditis (34, 35), and have in past studies shown development of significant chronic myocardial injury but represent a much more robust phenotype compared to A/J mice, we did hypothesize that immunoproteasome inhibition might also mitigate acute myocarditis in this breed and thereby subsequently lead to decreased incidence of cardiac tissue scarring, as is typical for ongoing chronic myocarditis. Because of their resilience to enterovirus infection when compared to A/J mice, who succumb to the infection in large numbers if not treated, NMRI mice appeared more suited to investigate a therapeutic approach over a longer period of time - however, leading on from our discovery of a possible positive effect for this breed when keeping immunoproteasome function intact, our research plan adapted accordingly.

Generally, in our experiments NMRI mice did not show the same clear-cut picture between ONX 0914 and vehicle-treated groups as was previously observed in the A/J breed regarding to their inflammatory phenotype induced by CVB3-myocarditis. Thereby their overall moderate inflammatory response may have contributed significantly as disease outcome for myocarditis has been shown to depend greatly on the scale of immune response activation in heart muscle tissue (36).

Compared to A/J mice, we did not find a nearly as impressive activation of pro-inflammatory cytokines and chemokines in NMRI mice, and histopathological comparison as well as analysis of immune cell infiltration showed less-pronounced

pathology in NMRI mice with unhindered immunoproteasome expression. This is in line with other published results showing that severe pathology is found mostly in accordance with high levels of cytokines and chemokines (2).
In addition to pharmaceutical inhibition by ONX 0914, genetic ablation of the immunoproteasome by ß5i/LMP7 knock-out can also be achieved. In A/J mice, this knock-out is well characterized and generally compensated for by an increased formation of standard proteasome, as shown by Opitz et al (37). On the contrary, for LMP7-deficient B6 mice, several studies show that intact immunoproteasome function is centrally important in regard to maintenance of protein homeostasis by degradation of damaged intracellular proteins in an inflammatory context (13, 38). For NMRI mice, to date, no LMP7 knock-out has been created, limiting our understanding of this breeds innate and adaptive immune response to enterovirus myocarditis in the context of immunoproteasome function to the use of inhibitors like ONX 0914. It has however been suggested that the different mouse breeds used to investigate the immunopathology of acute and chronic viral myocarditis, represent a diversity found in humans who display varying susceptibility to the disease as well.

4.3 Embedding the results into the current state of research

Leading on from the results described here and previously published by our group, some questions remain unanswered as new questions are raised.
Firstly, as our experiments presented in this study signify more of a characterisation of the NMRIs breed inflammatory reaction to the application of ONX 0914 during CVB3-myocarditis, and although we believe that our results show important new information regarding to an unexpected exacerbation of immunopathology by immunoproteasome dysfunction in a susceptible host during viral inflammatory heart disease, the question remains of how immunoproteasome function influences immune reaction and alters the course of infection in NMRI mice. While we have shown CVB3-triggered and significantly higher immune cell infiltration in immunoproteasome-disabled NMRI hearts, our upstream findings regarding to cytokine and chemokine levels do not serve to explain these findings molecularly. In A/J mice, we did previously find that application of ONX 0914 dampened the cytokine and chemokine release with significantly reduced levels for nearly all pro-inflammatory markers investigated and explaining why these animals benefitted from immunoproteasome blockade. Conclusively a much closer

look into NMRIs immunological make-up with and without the influence of ONX 0914 as well as release of cytokines and chemokines that govern immune cell differentiation is needed to explain the findings described in this study.

Additionally, looking at what is known about immune response during viral myocarditis for different mouse strains, as previously described, B6 mice that were re-challenged with CVB3 post primary infection exhibited no signs of re-infection and thereby no negative effect of ONX 0914 treatment on the development and maintenance of an intact immune response including memory status even though in this breed, a positive effect for intact immunoproteasome function was reported (7). We did not re-challenge NMRI mice to investigate whether they, like B6 mice, mount an intact immune response regarding memory function, unhindered by application of ONX 0914. Our results do however show that in FACS analysis of immune cell markers in heart tissue of NMRI mice treated with ONX 0914, inflammatory monocytes are found at significantly higher levels compared to vehicle-treated animals. In 2015 Leuschner et al (39) found that high peripheral cell counts of macrophages and monocytes contribute to more severe pathology in the cardiac inflammatory context, and this was attributed at least in part to ONX 0914 mobilisation of these cells from bone marrow.

Leading on from this and encompassing our results in NMRI mice, their phenotype of acute as well as chronic myocarditis in these experiments was not nearly as accentuated as in A/J mice. Although NMRI mice might experimentally represent a part of the population not primarily susceptible to a severe course of infection, in the end and regarding to a future bench-to-bedside approach with immunoproteasome inhibitors, A/J mice could be more suited to investigate viral cardiac inflammatory disease by CVB3 infection. Additionally, as the immunological make-up of NMRI mice is still not well characterized, further research into immunoproteasome and standard proteasome function in an inflammatory context is needed in future.

4.4 Strengths and weaknesses of the study

As with any experimental approach, conclusions drawn from a handful of experiments can never hope to finitely answer all questions pertaining to a research question. However, herein we provide compelling evidence that, contrary to previously published studies using different mouse breeds, pharmaceutical immunoproteasome inhibition does not protect NMRI mice from development of viral myocarditis, nor does it serve

to mitigate the course of disease. Rather, we have shown that keeping immunoproteasome function intact leads to decreased viral burden, lessens myocyte destruction and reduces the numbers of infiltrating immune cells into heart muscle tissue. This may be explained in part by a loss of efficacy for ONX 0914 in heart tissue during the course of infection. As with other mouse studies done by our group, we have kept the study designs and overall experimental plans the same, allowing us to compare our results using different breeds in the past. The methods used here for infection of mice with CVB3, virus dosage and treatment with ONX 0914, as well as the handling and storage of the inhibitor have been well established and thereby repeatedly internally validated in our group. While a total of three *in vivo* experiments provided the main data generated and presented here, the *in vitro* analysis of this data was meticulously planned and executed as well as repeated at least three times. This of course does not pertain to FACS analysis and echocardiography studies, as these would require more animals. In line with the 3R-guidelines issued by the Charité, great care was taken not to carelessly repeat *in vivo* experiments where unnecessary. However, this of course does lend itself to the fact that the phenotype described and observed in this study is much less pronounced, simply because the breed itself is more robust. Would larger groups of animals have been used, one could hypothesize that the effects seen would be more significant and that there might be effects not seen in our set-up. Seeing as most of our results do align with observations made by others as well and can be discussed in reference to well-published studies, we deem our group size as large enough to observe the most pronounced effects.
Additionally, a number of experiments regarding to the upstream effects of ONX 0914 in NMRI mice would have been very interesting, seeing as this phenotype as yet is not well-described. In future studies, in-depth system biology-based approaches would be needed to further our understanding of the immunoproteasomes role in this inflammatory context.

5. Conclusions

In summary, the data presented in this study shows that while NMRI mice do develop both acute and as previously described, chronic viral myocarditis, blockade of the immunoproteasome leads to aggravated inflammatory response, including higher numbers of infiltrating immune cells in the heart, increased cardiomyocyte death and

impaired virus control. This may be attributed to direct viral cytotoxicity, as secondary lymphatic tissues with high baseline immunoproteasome expression such as the spleen did not show signs of higher viral load in ONX 0914-treated animals. Additionally, we found that application of ONX 0914 showed a loss of efficacy for inhibition of the immunoproteasome subunit LMP7 and did bind a significant proportion of standard subunit ß5 as well, representative of diminished isoform selectivity over time – for treatment over longer periods of time, this could well result in disturbed protein homeostasis and subsequent proteotoxic stress in tissues with high abundance of standard proteasome and low baseline immunoproteasome expression, giving way to cardiotoxic side effects. Our results herein are reminiscent of data obtained for viral myocarditis in B6 mice, who also experience inhibition of the innate antiviral immune response resulting in increased immunopathology upon application of ONX 0914.

Overall, we would argue in favor of keeping immunoproteasome function intact in this model of viral myocarditis. However, in studies published by our group in recent years, data for A/J mice show a significant protective effect for ONX 0914, given prior to virus inoculation, mitigating an overwhelming, sepsis-like phenotype in this breed. Finally, we conclude that while immunoproteasome inhibition significantly influences immunopathology in mouse models of viral myocarditis, future utilisation of immunoproteasome inhibitors such as ONX 0914 would be hindered by the need for application prior to the onset of the systemic inflammatory response.

Reference list

1. Collaborators GBoDS. Global, regional, and national incidence, prevalence, and years lived with disability for 301 acute and chronic diseases and injuries in 188 countries, 1990–2013: a systematic analysis for the Global Burden of Disease Study 2013. The Lancet. 2015;386(9995):743-800.
2. Corsten MF, Schroen B, Heymans S. Inflammation in viral myocarditis: friend or foe? Trends Mol Med. 2012;18(7):426-37.
3. Cohle SD, Lie JT. Myasthenia gravis-associated systemic vasculitis and myocarditis with involvement of the cardiac conducting tissue. Cardiovasc Pathol. 1996;5(3):159-62.
4. Bechman K, Gopalan D, Nihoyannopoulos P, Mason JC. A cohort study reveals myocarditis to be a rare and life-threatening presentation of large vessel vasculitis. Semin Arthritis Rheum. 2017;47(2):241-6.
5. Moslehi JJ, Salem JE, Sosman JA, Lebrun-Vignes B, Johnson DB. Increased reporting of fatal immune checkpoint inhibitor-associated myocarditis. Lancet. 2018;391(10124):933.
6. Grandin EW, Ky B, Cornell RF, Carver J, Lenihan DJ. Patterns of cardiac toxicity associated with irreversible proteasome inhibition in the treatment of multiple myeloma. J Card Fail. 2015;21(2):138-44.
7. Althof N, Goetzke CC, Kespohl M, Voss K, Heuser A, Pinkert S, Kaya Z, Klingel K, Beling A. The immunoproteasome-specific inhibitor ONX 0914 reverses susceptibility to acute viral myocarditis. EMBO Mol Med. 2018;10(2):200-18.
8. Neumann DA, Rose NR, Ansari AA, Herskowitz A. Induction of multiple heart autoantibodies in mice with coxsackievirus B3- and cardiac myosin-induced autoimmune myocarditis. J Immunol. 1994;152(1):343-50.
9. Klingel K, Hohenadl C, Canu A, Albrecht M, Seemann M, Mall G, Kandolf R. Ongoing enterovirus-induced myocarditis is associated with persistent heart muscle infection: quantitative analysis of virus replication, tissue damage, and inflammation. Proc Natl Acad Sci U S A. 1992;89(1):314-8.
10. Kallewaard NL, Zhang L, Chen JW, Guttenberg M, Sanchez MD, Bergelson JM. Tissue-specific deletion of the coxsackievirus and adenovirus receptor protects

mice from virus-induced pancreatitis and myocarditis. Cell Host Microbe. 2009;6(1):91-8.
11. Wessely R, Klingel K, Santana LF, Dalton N, Hongo M, Jonathan Lederer W, Kandolf R, Knowlton KU. Transgenic expression of replication-restricted enteroviral genomes in heart muscle induces defective excitation-contraction coupling and dilated cardiomyopathy. J Clin Invest. 1998;102(7):1444-53.
12. Neumaier HL, Harel S, Klingel K, Kaya Z, Heuser A, Kespohl M, Beling A. ONX 0914 Lacks Selectivity for the Cardiac Immunoproteasome in CoxsackievirusB3 Myocarditis of NMRI Mice and Promotes Virus-Mediated Tissue Damage. Cells. 2020;9(5).
13. Ebstein F, Voigt A, Lange N, Warnatsch A, Schroter F, Prozorovski T, Kuckelkorn U, Aktas O, Seifert U, Kloetzel PM, Kruger E. Immunoproteasomes are important for proteostasis in immune responses. Cell. 2013;152(5):935-7.
14. Thrower JS, Hoffman L, Rechsteiner M, Pickart CM. Recognition of the polyubiquitin proteolytic signal. EMBO J. 2000;19(1):94-102.
15. Hershko A, Ciechanover A. The ubiquitin system. Annu Rev Biochem. 1998;67:425-79.
16. Ciechanover A. The unravelling of the ubiquitin system. Nat Rev Mol Cell Biol. 2015;16(5):322-4.
17. Carrell RW, Lomas DA. Conformational disease. Lancet. 1997;350(9071):134-8.
18. Bucciantini M, Giannoni E, Chiti F, Baroni F, Formigli L, Zurdo J, Taddei N, Ramponi G, Dobson CM, Stefani M. Inherent toxicity of aggregates implies a common mechanism for protein misfolding diseases. Nature. 2002;416(6880):507-11.
19. Medicherla B, Goldberg AL. Heat shock and oxygen radicals stimulate ubiquitin-dependent degradation mainly of newly synthesized proteins. J Cell Biol. 2008;182(4):663-73.
20. Aki M, Shimbara N, Takashina M, Akiyama K, Kagawa S, Tamura T, Tanahashi N, Yoshimura T, Tanaka K, Ichihara A. Interferon-gamma induces different subunit organizations and functional diversity of proteasomes. J Biochem. 1994;115(2):257-69.

21. Szalay G, Meiners S, Voigt A, Lauber J, Spieth C, Speer N, Sauter M, Kuckelkorn U, Zell A, Klingel K, Stangl K, Kandolf R. Ongoing coxsackievirus myocarditis is associated with increased formation and activity of myocardial immunoproteasomes. Am J Pathol. 2006;168(5):1542-52.
22. McCarthy MK, Malitz DH, Molloy CT, Procario MC, Greiner KE, Zhang L, Wang P, Day SM, Powell SR, Weinberg JB. Interferon-dependent immunoproteasome activity during mouse adenovirus type 1 infection. Virology. 2016;498:57-68.
23. Kincaid EZ, Che JW, York I, Escobar H, Reyes-Vargas E, Delgado JC, Welsh RM, Karow ML, Murphy AJ, Valenzuela DM, Yancopoulos GD, Rock KL. Mice completely lacking immunoproteasomes show major changes in antigen presentation. Nat Immunol. 2011;13(2):129-35.
24. Basler M, Dajee M, Moll C, Groettrup M, Kirk CJ. Prevention of experimental colitis by a selective inhibitor of the immunoproteasome. J Immunol. 2010;185(1):634-41.
25. Mundt S, Engelhardt B, Kirk CJ, Groettrup M, Basler M. Inhibition and deficiency of the immunoproteasome subunit LMP7 attenuates LCMV-induced meningitis. Eur J Immunol. 2016;46(1):104-13.
26. Bockstahler M, Fischer A, Goetzke CC, Neumaier HL, Sauter M, Kespohl M, Muller AM, Meckes C, Salbach C, Schenk M, Heuser A, Landmesser U, Weiner J, Meder B, Lehmann L, Kratzer A, Klingel K, Katus HA, Kaya Z, Beling A. Heart-Specific Immune Responses in an Animal Model of Autoimmune-Related Myocarditis Mitigated by an Immunoproteasome Inhibitor and Genetic Ablation. Circulation. 2020;141(23):1885-902.
27. Mundt S, Basler M, Buerger S, Engler H, Groettrup M. Inhibiting the immunoproteasome exacerbates the pathogenesis of systemic Candida albicans infection in mice. Sci Rep. 2016;6:19434.
28. Mundt S, Basler M, Sawitzki B, Groettrup M. No prolongation of skin allograft survival by immunoproteasome inhibition in mice. Mol Immunol. 2017;88:32-7.
29. Grosicki S, Barchnicka A, Jurczyszyn A, Grosicka A. Bortezomib for the treatment of multiple myeloma. Expert Rev Hematol. 2014;7(2):173-85.

30. Norwood TG, Westbrook BC, Johnson DB, Litovsky SH, Terry NL, McKee SB, Gertler AS, Moslehi JJ, Conry RM. Smoldering myocarditis following immune checkpoint blockade. J Immunother Cancer. 2017;5(1):91.
31. Wei SC, Meijers WC, Axelrod ML, Anang NAS, Screever EM, Wescott EC, Johnson DB, Whitley E, Lehmann L, Courand PY, Mancuso JJ, Himmel LE, Lebrun-Vignes B, Wleklinski MJ, Knollmann BC, Srinivasan J, Li Y, Atolagbe OT, Rao X, Zhao Y, Wang J, Ehrlich LIR, Sharma P, Salem JE, Balko JM, Moslehi JJ, Allison JP. A genetic mouse model recapitulates immune checkpoint inhibitor-associated myocarditis and supports a mechanism-based therapeutic intervention. Cancer Discov. 2020.
32. Goetzke CC, Althof N, Neumaier HL, Heuser A, Kaya Z, Kespohl M, Klingel K, Beling A. Mitigated viral myocarditis in A/J mice by the immunoproteasome inhibitor ONX 0914 depends on inhibition of systemic inflammatory responses in CoxsackievirusB3 infection. Basic Res Cardiol. 2021;116(1):7.
33. Kumar R, Mehta D, Mishra N, Nayak D, Sunil S. Role of Host-Mediated Post-Translational Modifications (PTMs) in RNA Virus Pathogenesis. Int J Mol Sci. 2020;22(1).
34. Merkle I, Tonew M, Gluck B, Schmidtke M, Egerer R, Stelzner A. Coxsackievirus B3-induced chronic myocarditis in outbred NMRI mice. J Hum Virol. 1999;2(6):369-79.
35. Schmidtke M, Merkle I, Klingel K, Hammerschmidt E, Zautner AE, Wutzler P. The viral genetic background determines the outcome of coxsackievirus B3 infection in outbred NMRI mice. J Med Virol. 2007;79(9):1334-42.
36. Kindermann I, Kindermann M, Kandolf R, Klingel K, Bultmann B, Muller T, Lindinger A, Bohm M. Predictors of outcome in patients with suspected myocarditis. Circulation. 2008;118(6):639-48.
37. Opitz E, Koch A, Klingel K, Schmidt F, Prokop S, Rahnefeld A, Sauter M, Heppner FL, Volker U, Kandolf R, Kuckelkorn U, Stangl K, Kruger E, Kloetzel PM, Voigt A. Impairment of immunoproteasome function by beta5i/LMP7 subunit deficiency results in severe enterovirus myocarditis. PLoS Pathog. 2011;7(9):e1002233.

38. Seifert U, Bialy LP, Ebstein F, Bech-Otschir D, Voigt A, Schroter F, Prozorovski T, Lange N, Steffen J, Rieger M, Kuckelkorn U, Aktas O, Kloetzel PM, Kruger E. Immunoproteasomes preserve protein homeostasis upon interferon-induced oxidative stress. Cell. 2010;142(4):613-24.
39. Leuschner F, Courties G, Dutta P, Mortensen LJ, Gorbatov R, Sena B, Novobrantseva TI, Borodovsky A, Fitzgerald K, Koteliansky V, Iwamoto Y, Bohlender M, Meyer S, Lasitschka F, Meder B, Katus HA, Lin C, Libby P, Swirski FK, Anderson DG, Weissleder R, Nahrendorf M. Silencing of CCR2 in myocarditis. Eur Heart J. 2015;36(23):1478-88.

Statutory Declaration

“I, Hannah Louise Neumaier, by personally signing this document in lieu of an oath, hereby affirm that I prepared the submitted this dissertation on the topic “Targeting proteolysis in viral cardiac inflammatory disease/ Einfluss der Proteolyse auf Virus-assoziierte entzündliche Herzmuskelerkrankungen” independently and without the support of third parties, and that I used no other sources and aids than those stated. All parts which are based on the publications or presentations of other authors, either in letter or in spirit, are specified as such in accordance with the citing guidelines. The sections on methodology (in particular regarding practical work, laboratory regulations, statistical processing) and results (in particular regarding figures, charts and tables) are exclusively my responsibility.

Furthermore, I declare that I, Hannah Louise Neumaier, have correctly marked all of the data, the analyses, and the conclusions generated from data obtained in collaboration with other persons, and that I have correctly marked my own contribution and the contributions of other persons (cf. declaration of contribution). I have correctly marked all texts or parts of texts that were generated in collaboration with other persons.

My contributions to any publications to this dissertation correspond to those stated in the below joint declaration made together with the supervisor. All publications created within the scope of the dissertation comply with the guidelines of the ICMJE (International Committee of Medical Journal Editors; http://www.icmje.org) on authorship. In addition, I declare that I shall comply with the regulations of Charité – Universitätsmedizin Berlin on ensuring good scientific practice.

I declare that I have not yet submitted this dissertation in identical or similar form to another Faculty.

The significance of this statutory declaration and the consequences of a false statutory declaration under criminal law (Sections 156, 161 of the German Criminal Code) are known to me.”

Date Signature

Declaration of my own contribution to the publication

After an initial introduction into the laboratory processes and into the topic, I procured a M.D. scholarship provided by the Berlin Institute of Health to be able to work on this project exclusively for 12 months. Additionally, I have spent 1,5 more years in and with the project, analyzing and curating data as well as writing my parts of our publications and this dissertation. A point by point overview of contributions to the data shown in this dissertation is provided in the table below.

Own Publication:

Hannah Louise Neumaier, Shelly Harel, Karin Klingel, Ziya Kaya, Arnd Heuser, Meike Kespohl and Antje Beling: ONX 0914 lacks selectivity for the cardiac immunoproteasome in CoxsackievirusB3 myocarditis of NMRI mice and promotes virus-mediated tissue damage. Cells, 2020 May 9(5): 1093, published online 2020 Apr 28, doi: 10.3390/cells9051093

I contributed to this publication as follows:
Together with Meike Kespohl, I established methods for the experimental mouse model with NMRI mice at our lab, explicitly for experiments included in figures 1, 2 and 3. Echocardiography was performed by Arnd Heuser's Team while analysis of raw data from the examination (shown in tables 1 and 2) was done by me.
I planned and carried out all experiments with the help of Antje Beling, except those included in figures 4 and 5 which were in part executed by Shelly Harel. All data shown in figures 1, 2 and 3 as well as tables 1 and 2 was curated, formally and statistically analyzed by me with the exception of histology shown in figures 1, 2 and 3 which was analyzed by Karin Klingel. Technical assistance was provided by K. Voß for all experiments and especially regarding to animal experiments and qPCR data in figure 4F.
I validated data pertaining to all figures shown (figures 4 and 5 together with Shelly Harel) and wrote the original manuscript together with Antje Beling.

Data shown in this dissertation:

Data shown	Type of analysis	Collection of samples	Raw data generation	Data analysis and interpretation
Figure 1	Establishment of experimental schedules and histological analysis	(A)-(D) H.Neumaier	(A)-(C) H. Neumaier (D) K.Klingel	(A)-(C) H.Neumaier, M. Kespohl, A. Beling (D) K.Klingel
Table 1	Echocardiography	-	Ultrasound performed by the Heuser group (MDC Berlin)	H.Neumaier, A.Beling
Figure 2	(A) mRNA qPCR (B) histology (C) microscopic images	(A)-(C) H.Neumaier	(A) H.Neumaier (B) K.Klingel (C) K.Klingel	(A) H.Neumaier (B) H.Neumaier (C) K.Klingel
Figure 3	(A) histology (B) mRNA qPCR (C) FACS (D) histology	(A)-(D) H.Neumaier	(A) K.Klingel (B) +(C) H.Neumaier (D) K.Klingel	(A) -(C) H.Neumaier (D) K.Klingel
Figure 4	(A) histology (B) mRNA qPCR (C) hsTnT (D) microscopic images (E) FACS (F) mRNA expression	(A)-(F) H.Neumaier	(A) K.Klingel (B) H.Neumaier (C) measurements provided by the Kaya group (University of Heidelberg) (D) K.Klingel (E) -(F) H.Neumaier	(A) -(C) H.Neumaier (D) K.Klingel (E)-(F) H.Neumaier
Table 2	Echocardiography	-	Ultrasound performed by the Heuser group (MDC Berlin)	H.Neumaier, A.Beling
Figure 5	(A) +(B) mRNA qPCR (C)+(D) Western blot (E)+(F) mRNA qPCR	(A)-(F) H.Neumaier	(A) +(B) H.Neumaier, S.Harel (C)+(D) H.Neumaier (E)+(F) H.Neumaier, S.Harel	(A)-(F) H.Neumaier, S.Harel

_____

Unterschrift, Datum und Stempel der erstbetreuenden Hochschullehrerin

_____

Unterschrift der Doktorandin

Excerpt from the Journal Summary List

Journal Data Filtered By: **Selected JCR Year: 2018** Selected Editions: SCIE,SSCI
Selected Categories: **"CELL BIOLOGY"** Selected Category Scheme: WoS
Gesamtanzahl: 193 Journale

Rank	Full Journal Title	Total Cites	Journal Impact Factor	Eigenfactor Score
1	NATURE REVIEWS MOLECULAR CELL BIOLOGY	45,869	43.351	0.091360
2	CELL	242,829	36.216	0.571850
3	NATURE MEDICINE	79,243	30.641	0.162840
4	CANCER CELL	36,056	23.916	0.091050
5	Cell Metabolism	34,829	22.415	0.099550
6	Cell Stem Cell	24,628	21.464	0.087030
7	CELL RESEARCH	15,131	17.848	0.038680
8	NATURE CELL BIOLOGY	40,615	17.728	0.082430
9	Science Translational Medicine	30,485	17.161	0.121980
10	TRENDS IN CELL BIOLOGY	14,380	16.588	0.034120
11	MOLECULAR CELL	62,812	14.548	0.170680
12	NATURE STRUCTURAL & MOLECULAR BIOLOGY	27,166	12.109	0.069440
13	EMBO JOURNAL	65,212	11.227	0.067930
14	Autophagy	16,161	11.059	0.032630
15	TRENDS IN MOLECULAR MEDICINE	9,946	11.028	0.018900
16	Journal of Extracellular Vesicles	3,675	11.000	0.012110
17	Annual Review of Cell and Developmental Biology	9,734	10.833	0.016750
18	AGEING RESEARCH REVIEWS	6,539	10.390	0.015890
19	CURRENT BIOLOGY	60,772	9.193	0.135820
20	DEVELOPMENTAL CELL	28,572	9.190	0.068550

Rank	Full Journal Title	Total Cites	Journal Impact Factor	Eigenfactor Score
21	Cold Spring Harbor Perspectives in Biology	15,375	9.110	0.041830
22	GENES & DEVELOPMENT	54,563	8.990	0.072340
23	JOURNAL OF CELL BIOLOGY	67,347	8.891	0.075660
24	Cell Systems	2,275	8.640	0.016280
25	PLANT CELL	52,034	8.631	0.057800
26	EMBO REPORTS	13,786	8.383	0.029850
27	CURRENT OPINION IN CELL BIOLOGY	13,417	8.233	0.025790
28	CELL DEATH AND DIFFERENTIATION	19,729	8.086	0.030290
29	Cell Reports	39,510	7.815	0.235540
30	Protein & Cell	3,243	7.575	0.009080
31	AGING CELL	8,993	7.346	0.018810
32	CURRENT OPINION IN STRUCTURAL BIOLOGY	11,066	7.052	0.024160
33	CELLULAR AND MOLECULAR LIFE SCIENCES	24,422	7.014	0.038970
34	MATRIX BIOLOGY	5,699	6.986	0.009540
35	ONCOGENE	63,249	6.634	0.074600
36	Tissue Engineering Part B-Reviews	3,550	6.512	0.004970
37	Science Signaling	11,403	6.481	0.033700
38	Cell Death & Disease	19,001	5.959	0.051780
39	Signal Transduction and Targeted Therapy	371	5.873	0.000990
40	Cells	1,412	5.656	0.003990
41	STEM CELLS	21,467	5.614	0.030220
42	Aging-US	5,185	5.515	0.012440

Selected JCR Year: 2018; Selected Categories: "CELL BIOLOGY"

from: *Journal Citation Reports 2018,* category „Cell Biology“, paper published in nr. 40 *Cells* (see red mark), *Impact Faktor: 5.656*

cells

MDPI

Article

ONX 0914 Lacks Selectivity for the Cardiac Immunoproteasome in CoxsackievirusB3 Myocarditis of NMRI Mice and Promotes Virus-Mediated Tissue Damage

Hannah Louise Neumaier [1], Shelly Harel [1], Karin Klingel [2], Ziya Kaya [3,4], Arnd Heuser [5], Meike Kespohl [1,6] and Antje Beling [1,6,*]

1 Charité—Universitätsmedizin Berlin, Corporate Member of Freie Universität Berlin, Humboldt-Universität zu Berlin, and Berlin Institute of Health (BIH), Institute of Biochemistry, 10117 Berlin, Germany; hannah-louise.neumaier@charite.de (H.L.N.); shellyharel@web.de (S.H.); meike.kespohl@charite.de (M.K.)
2 Institute for Cardiopathology, University of Tuebingen, 72074 Tuebingen, Germany; karin.klingel@med.uni-tuebingen.de
3 Medizinische Klinik für Innere Medizin III: Kardiologie, Angiologie und Pneumologie, Universitätsklinikum Heidelberg, Medizinische Klinik für Innere Medizin III: Kardiologie, Angiologie und Pneumologie, Universitätsklinikum Heidelberg, 69120 Heidelberg, Germany; ziya.kaya@med.uni-heidelberg.de
4 Deutsches Zentrum für Herz-Kreislauf-Forschung (DZHK), partner side Heidelberg/Mannheim, 69120 Heidelberg, Germany
5 Max-Delbrueck-Center for Molecular Medicine, 10115 Berlin, Germany; heuser@mdc-berlin.de
6 Deutsches Zentrum für Herz-Kreislauf-Forschung (DZHK), partner side Berlin, 10785 Berlin, Germany
* Correspondence: antje.beling@charite.de

Received: 30 January 2020; Accepted: 23 April 2020; Published: 28 April 2020

Abstract: Inhibition of proteasome function by small molecules is highly efficacious in cancer treatment. Other than non-selective proteasome inhibitors, immunoproteasome-specific inhibitors allow for specific targeting of the proteasome in immune cells and the profound anti-inflammatory potential of such compounds revealed implications for inflammatory scenarios. For pathogen-triggered inflammation, however, the efficacy of immunoproteasome inhibitors is controversial. In this study, we investigated how ONX 0914, an immunoproteasome-selective inhibitor, influences CoxsackievirusB3 infection in NMRI mice, resulting in the development of acute and chronic myocarditis, which is accompanied by formation of the immunoproteasome in heart tissue. In groups in which ONX 0914 treatment was initiated once viral cytotoxicity had emerged in the heart, ONX 0914 had no anti-inflammatory effect in the acute or chronic stages. ONX 0914 treatment initiated prior to infection, however, increased viral cytotoxicity in cardiomyocytes, promoting infiltration of myeloid immune cells into the heart. At this stage, ONX 0914 completely inhibited the β5 subunit of the standard cardiac proteasome and less efficiently blocked its immunoproteasome counterpart LMP7. In conclusion, ONX 0914 unselectively perturbs cardiac proteasome function in viral myocarditis of NMRI mice, reduces the capacity of the host to control the viral burden and promotes cardiac inflammation.

Keywords: myocarditis; proteasome; immunoproteasome inhibitor; inflammation; proteostasis

1. Introduction

The ubiquitin-proteasome system (UPS) is an integral part of cellular proteostasis, functioning as the primary route for intracellular degradation of misfolded, damaged, or short-lived proteins [1]. The ubiquitin conjugation machinery marks these proteins for recognition by the proteolytic complex, the proteasome. The proteasome is a barrel-shaped, twofold symmetric, multi-subunit enzyme that is

flanked by regulatory 19S regulatory particles (19S), which serve to bind protein substrates. Peptide hydrolysis is exclusively carried out by β1, β2, and β5 subunits within the inner chamber of the 20S core complex. Particularly under conditions of cellular stress, the UPS needs to adapt its protein turnover capacity to ensure elimination of the increasing abundance of unfolded and potentially toxic proteins [2]. In response to inflammatory cytokines [3,4], DNA-damage [5], or oxidative stress [6], cells selectively upregulate the expression of the immunoproteasome (i-proteasome), a specific proteasome isoform, containing alternative catalytic subunits (β1i/LMP2, β2i/MECL-1, β5i/LMP7) [7]. In comparison to its standard proteasome counterpart, the i-proteasome accelerates the proteolysis of specific peptide substrates [8,9] and allows for the facilitated degradation of oxidant-damaged proteins, which may accumulate during inflammation, for example [3,10,11]. While this specific adaptation of proteasome function is of particular relevance in non-immune cells with high standard proteasome abundance under basal conditions, immune cells exhibit high i-proteasome and low standard proteasome expression levels in their naive state. This cell-specific proteasome-isoform expression pattern in non-immune and immune cells initiated the structure-guided design of specific proteasome inhibitors, specifically targeting the i-proteasome [12,13].

Based on the IFN-γ-dependent upregulation of the i-proteasome subunits, which are in close proximity to the genes of the MHC II region, and their unique cleavage properties, the i-proteasome was initially seen as a prerequisite needed for efficient MHC class I antigen presentation [4,14]. Undisputedly, the i-proteasome strongly enhances $CD8^+$ T cell responses for some pathogens [15–17], yet there are also examples where the standard proteasome can efficiently compensate for the lack of intact i-proteasome activity [18,19]. Of the different compounds which can experimentally accomplish inhibition of the i-proteasome, ONX 0914 is the best characterized [20,21]. Whereas physiologically desired effects achieved by treatment with the epoxyketone ONX 0914 requires a combined inhibition of both LMP7 and LMP2 [20,21], there is also a LMP7-selective dipeptide inhibitor available which shows potent immunosuppressive activity [22]. Another compound referred to as PRN1126, developed as an exclusively LMP7-specific inhibitor shows, however, limited in vivo effects on adverse immune responses [21]. Nevertheless, the availability of selective i-proteasome inhibitors paved the way towards the definition of new functions of the i-proteasome. These involve control of DAMP- or PAMP-triggered signaling responses, resulting in elevated production of cytokines, e.g., by innate myeloid cells, altered T cell activation and differentiation, B cell function, or immune cell survival [23–25]. Based on these multidimensional immune cellular functions, it was expected that i-proteasome inhibitors would be capable of hindering inflammation-driven carcinogenesis [26,27], autoimmune-related inflammation [20,28,29], or transplant rejection [22,30].

Inhibiting the i-proteasome, however, in response to infection-triggered inflammation is a double-edged sword, since the repertoire of cellular processes affected by the i-proteasome ranges from proper immune cell activation needed for pathogen control to potentially harmful events, known as immunopathology. Particularly for intracellular pathogens, such as fungi, protozoa, viruses, or intracellular bacteria, which rely on successful MHC class I antigen presentation machinery for elimination of infected cells by $CD8^+$ T lymphocytes, this limits the general applicability of i-proteasome inhibitors for the treatment of pathogen-triggered inflammation [31,32]. Myocarditis, an inflammatory disease of the heart, is a classic example where both direct pathogen-mediated cellular injury, as well as the resulting activation of an immune response, contribute to acute organ failure and simultaneously predispose patients to chronic cardiac dysfunction [33]. Since in the Western world, non-ischemic cardiac inflammatory disease is most commonly caused by viral infections, our research group, which is interested in dissecting the pathology behind this disease, relies on the well-established mouse model of Coxsackievirus B3 (CVB3) myocarditis [33]. Infection with CVB3, a single-stranded RNA virus of the Picornaviridae family, and the immune response that follows, induce a sequence of organ-specific and systemic pathologies. Using the intraperitoneal inoculation route, the virus initially causes a pancreatitis, resulting in destruction of exocrine cells of the pancreas [34], and subsequently myocarditis, showing variable severity in different laboratory mouse strains [35]. Depending on the strain-specific

susceptibility to the disease, mice develop a heterogeneous acute [8,36] and sometimes a chronic stage of the disease [37], providing an opportunity for research into the development of chronic sequela, such as inflammatory cardiomyopathy, which can manifest after acute myocarditis. The i-proteasome plays an important, yet not fully explained role in the process of CVB3-triggered cardiac inflammatory immune response, with both knockout and inhibition of the multi-catalytic protease exacerbating the disease in C57BL/6 mice [3,38]. The i-proteasome is strongly upregulated in heart tissue during viral myocarditis and its induction involves type I IFNs [8] as well as IFN-γ [39]. In C57BL/6 mice, the i-proteasome is required for the timely degradation of oxidant-damaged proteins, to prevent their accumulation in inflamed cells and tissues [3,11,40]. Moreover, the i-proteasome regulates the production of innate immune regulators, such as pentraxin3 [41], with failure of such processes contributing to enhanced cardiac tissue damage. In a previous work, however, we demonstrated that ONX 0914 can act in the opposite manner, clearly protecting another laboratory strain, namely A/J mice, from developing CVB3 myocarditis. In this host, i-proteasome activity is detrimental, since the comparatively severe pathology triggered by CVB3 infection in this strain is primarily attributed to an overall adverse immune response, resulting in a sepsis-like cytokine storm and distributive shock condition, all of which can be mitigated by i-proteasome inhibitors [38].

The magnitude of the acute inflammatory injury, triggered in the heart by cardiotropic viruses, predisposes a host to cardiac remodeling processes that involve classical wound healing processes with the differentiation of myofibroblasts and fibrosis formation [33]. Shifting focus from acute towards the chronic stages of the disease, we questioned whether i-proteasome inhibitors could potentially provide a targeted solution for attenuating disease progression to chronic stages—for where there is reduced acute heart muscle damage, subsequent scarring and cardiac remodeling can be expected to be more limited as well [42]. Although the A/J strain has been noted to form chronic inflammatory lesions [43], mice become severely ill during acute myocarditis and can partially succumb to infection [44]. In our hands, A/J mice are not ideally suited to investigate the chronic state. NMRI mice, however, while susceptible to acute CVB3-myocarditis, show much less impact on their general well-being and have consistently been shown to develop chronic viral myocarditis [37,45], making them a favored model for later stages of the disease. Regarding the positive effects, ONX 0914 treatment demonstrated in acute myocarditis in A/J mice, we asked the question whether i-proteasome inhibition by ONX 0914 might attenuate the development and severity of chronic myocarditis in NMRI mice as well.

2. Results

2.1. Influence of ONX 0914 on Myocarditis in NMRI Mice

Our previous work demonstrated a protective effect of ONX 0914 on acute inflammatory tissue injury of the heart after infection of A/J mice with a cardiotropic CVB3 strain [38]. To investigate how ONX 0914 influences a late consequence of viral infection, we used a well-characterized and frequently used mouse model for chronic viral myocarditis, inoculating outbred NMRI mice with CVB3 strain 31-1-93 [37]. We applied a therapeutic approach, with the initiation of treatment on day 3 post-infection [46], once viral injury of the heart tissue has emerged. Mice were randomized to a control (vehicle-treated) or ONX 0914 (inhibitor-treated) group and received daily doses from day 3 until day 8. Thereafter, until read out on day 28, treatment was continued three times per week (Figure 1A). During chronic infection, animals treated with ONX 0914 showed a significantly slower recovery from the initial weight-loss which mice typically develop during acute viral infection (Figure 1B). Analysis of the virus concentration in infected heart tissue revealed similar viral RNA copy numbers in mice treated with ONX 0914 (Figure 1C), with no detection of infectious viral particles in either vehicle- or inhibitor-treated groups on day 28. Troponin T (TnT) levels, measured using serum drawn on day 28, showed values equal to those of uninfected controls, demonstrating that there is no ongoing myocardial tissue destruction at this stage of infection in ONX 0914-treated groups (data not shown).

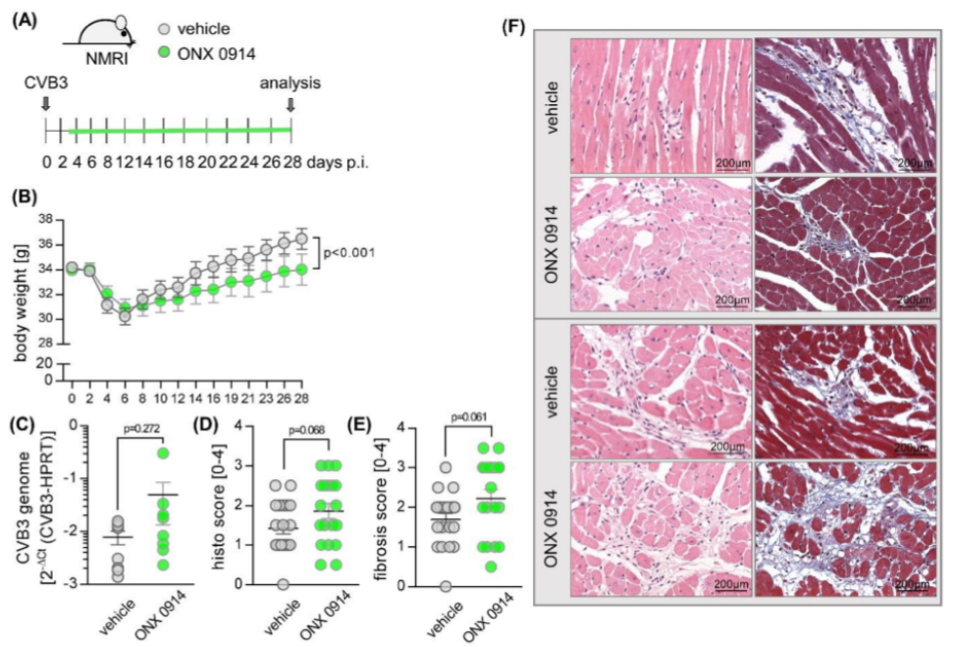

Figure 1. Effect of ONX 0914 on the manifestation of chronic viral myocarditis in NMRI mice. (**A**) Mice were inoculated with 5×10^5 pfu of Coxsackievirus B3 strain 31-1-93. Between days 3 and 8, mice were treated with ONX 0914 (5–10 mg/kg) or vehicle (Captisol) daily—thereafter treatment continued three times per week until day 28 (vehicle $n = 20$; ONX 0914 $n = 20$). (**B**) Body weight was monitored as indicated and analyzed using two-way ANOVA. (**C**) Mice were sacrificed after 28 days. RNA was extracted from heart tissue and Coxsackievirus B3 (CVB3) genome expression was determined by quantitative PCR. Paraffin-embedded, hematoxylin-eosin (**D**) and Masson's trichrome-stained cardiac tissue (**E**) was taken for histological scoring of cardiac injury and inflammation. (**F**) Two representative images (upper panel from the group treated with 5–7 mg/kg bodyweight ONX 0914; lower panel from the group treated with 10 mg/kg bodyweight ONX 0914) are shown for each treatment group. Data are mean ± SEM and analyzed by unpaired *t*-tests. *p*-values are indicated in each graph.

Echocardiography was performed to determine if there is any impact on cardiac function by ONX 0914 treatment (Table 1). Parameters that describe cardiac performance, such as cardiac output and ejection fraction of the left ventricle, were within the range of those detected in naive mice prior to infection, revealing no measurable influence due to ONX 0914 treatment. Altogether, these data provide evidence that post-viral cardiac remodeling, regardless of ONX 0914 treatment, has no biologically relevant effect on cardiac function in NMRI mice. Although the overall architecture of the heart muscle was not heavily affected, cardiac sections scored for cardiac remodeling processes, comprising post-viral inflammatory damage and formation of fibrosis, revealed signs of tissue injury (Figure 1D–F). Similar to the vehicle-treated group, ONX 0914 treatment led to elevated scores on day 28, clearly arguing against a protective effect of ONX 0914 on post-viral heart tissue injury in NMRI mice.

Since we found no functional deterioration at the chronic stage in infected NMRI mice, we asked how a therapeutic administration of ONX 0914 affects the virus-triggered inflammatory tissue damage during acute viral myocarditis, peaking at around day 8 post-infection, using NMRI mice. Similar to the first experiment, mice received ONX 0914 or the vehicle daily from day 3 after infection until day 8 (Figure 2A). During the course of acute infection up to day 8, ONX 0914 had no effect on body weight (Figure 2B). In ONX 0914-treated mice, we found a trend towards a slightly increased CVB3

concentration on day 8 post-infection (Figure 2C). Histological scoring of heart tissue, comprising myocardial necrosis and inflammation at this stage, revealed similar scores in both groups (Figure 2D/E). Overall, we found that ONX 0914 with treatment initiated after 3 days had no protective effects on acute viral myocarditis in NMRI mice. In fact, there was a tendency towards mild exacerbation of cardiac inflammation in the ONX 0914 group, which led us to ask whether the i-proteasome might, as shown for C57BL/6 mice [3,38,41], play a beneficial role during CVB3 myocarditis in NMRI mice.

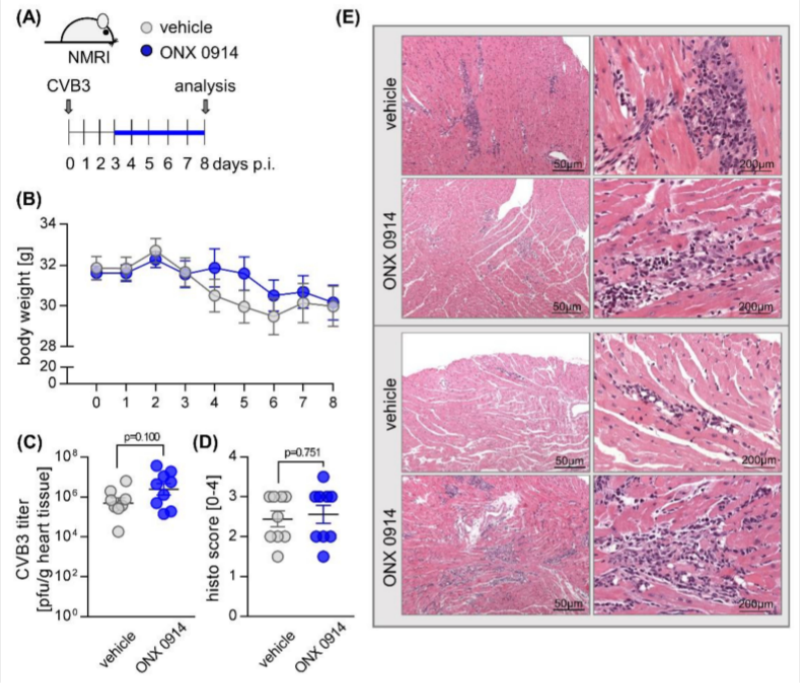

Figure 2. Effect of ONX 0914 on the manifestation of acute viral myocarditis in NMRI mice. (**A**) Mice were infected with 5×10^5 pfu CVB3 strain 31-1-93 (day 0). From day 3, mice received either ONX 0914 or vehicle daily until day 8. (**B**) Body weight was monitored as indicated. (**C**) Viral titers in hearts of both vehicle and ONX 0914-treated mice were determined by plaque assay. (**D**) Mice were then sacrificed, and heart tissue was analyzed microscopically for inflammation and fibrosis. (**E**) Histological images of two representative animals per group are shown. Data are summarized as mean ± SEM. Body weight was analyzed using two-way ANOVA, all remaining data were analyzed by unpaired *t*-tests.

To investigate the function of the i-proteasome in more depth, either ONX 0914 or vehicle was administered to mice daily for 8 days, starting one day prior to infection (Figure 3A), which ensured inhibition of the i-proteasome during the entire course of infection [38]. On day 0, mice were infected with CVB3. Regarding their overall body weight, there were no significant differences in the two treatment groups, with all mice experiencing weight loss, as is known for infection with CVB3 (Figure 3B). Measurement of serum TnT concentrations at day 8, however, revealed elevated TnT levels in inhibitor-treated animals in comparison to their controls, demonstrating that the myocardial injury was even more pronounced in those animals that were treated with ONX 0914 (Figure 3C). Correspondingly, histological scoring of HE-stained cardiac sections showed myocardial injury in ONX 0914-treated animals was, if anything, more severe (Figure 3D,E). Quantitative analysis of infiltrating immune cells, performed by flow cytometry of cardiac tissue, revealed a higher number

of inflammatory monocytes (Ly6C^{high}) in hearts obtained from ONX 0914-treated mice (Figure 3F). In viral myocarditis, the virus concentration and the cytotoxicity it induces is a main determinant for the severity of the inflammatory response. Both the evidence for greater myocardial tissue injury and the elevated number of myeloid immune cells in the heart tissue of ONX 0914-treated NMRI mice suggest that ONX 0914 influences the virus concentration in this host. In fact, we found that the viral load, as determined by quantitative PCR and plaque assay, was increased in mice treated with ONX 0914 in comparison to their controls (Figure 3H,I). Viral RNA is a classical trigger of IFN and cytokine production and we thus investigated how ONX 0914 influences the expression of these molecules in infected heart tissue. In ONX 0914-treated mice, we found an elevated IFN-β production, yet an unaffected IFN-stimulated gene signature as representatively shown by IFIT1 and IFIT3 expression. With the exception of CXCL-10, where ONX 0914 treatment resulted in higher expression levels, the mRNA expression of pro-inflammatory and chemoattractant cytokines was not affected by ONX 0914 treatment (Figure 3J).

Table 1. Analysis of cardiac function in NMRI mice during chronic myocarditis.

Collumn Name	Vehicle		ONX 0914	
	Baseline	**Day 28**	**Baseline**	**Day 28**
Heart rate (bpm)	417 ± 18	440 ± 18	440 ± 18	426 ± 14
Trace EF (%)	46 ± 2.5	48.1 ± 2.9	43.6 ± 2.6	42.7 ± 2.0
Cardiac output (mL/min)	13.6 ± 1.0	14.6 ± 1.0	14.3 ± 1.1	14.0 ± 0.8
Stroke volume (µL)	32.4 ± 1.8	32.7 ± 1.5	32.0 ± 1.9	33.0 ± 1.8
Vol d (µL)	70.5 ± 1.7	70.0 ± 3.1	74.2 ± 3	77.0 ± 2.2
Vol s (µL)	38.1 ± 1.9	37.3 ± 3.0	42.2 ± 2.9	44.2 ± 2.0
LVID-d (mm)	4.3 ± 0.1	4.3 ± 0.1	4.3 ± 0.1	4.5 ± 0.1
LVID-s (mm)	3.2 ± 0.1	3.1 ± 0.1	3.2 ± 0.1	3.5 ± 0.1

Echocardiography was performed prior to infection (day 0) and on day 28 post-infection. After infection, mice received ONX 0914, starting on day 3 (n = 20 ONX 0914). Age- and gender-matched vehicle-treated mice served as controls (n = 20 vehicle). Data shown are mean values ± SEM and were analyzed using repeated measurements two-way ANOVA, yielding no significant changes. EF = ejection fraction; bpm = beats per minute; Vol d/s = end-diastolic/-systolic left ventricular volume; LVID-d/s = left ventricular diameter at diastole/systole.

To investigate how ONX 0914 treatment in acute myocarditis influences ventricular filling, vascular tone, and resultant cardiac performance, we performed echocardiography (Table 2).

Table 2. Analysis of cardiac function in NMRI mice during acute myocarditis.

	Vehicle		ONX 0914	
	Baseline	**Day 8**	**Baseline**	**Day 8**
Heart rate (bpm)	427 ± 16	393 ± 16	500 ± 13 *	405 ± 23 §
Trace EF (%)	50.7 ± 1.7	48.4 ± 2.6	57.4 ± 2.3	49.1 ± 3.2 §
Cardiac output (mL/min)	14.4 ± 1.2	10.0 ± 0.9 §	18.6 ± 1.2 *	12.1 ± 1.3 §
Stroke volume (µL)	33.6 ± 2.1	25.2 ± 1.4 §	37.3 ± 2.4	29.6 ± 2.3 §
Vol d (µL)	66.5 ± 4.0	52.8 ± 3.0 §	65.5 ± 4.0	60.3 ± 2.6
Vol s (µL)	33.0 ± 2.4	27.6 ± 2.6	28.1 ± 2.5	30.7 ± 2.3
LVID-d (mm)	4.2 ± 0.1	4.0 ± 0.1	4.2 ± 0.1	4.2 ± 0.1
LVID-s (mm)	3.1 ± 0.1	3.0 ± 0.1	2.9 ± 0.1	3.2 ± 0.1

ONX 0914 (10 mg/kg BW) was initiated in naive NMRI mice one day prior to infection. Echocardiography was performed at baseline (day 0) and on day 8 post-infection. Age- and gender-matched vehicle-treated littermates served as controls (n = 10 vehicle and n = 10 ONX 0914). Data shown are mean values ± SEM and were analyzed using repeated measurements two-way ANOVA, followed by Sidak's multiple comparison test. § indicates significant differences in the respective treatment group at day 8 compared to this groups' baseline measurement. * indicates significant differences regarding ONX 0914 treatment prior to infection. EF = ejection fraction; bpm = beats per minute; Vol d/s = end-diastolic/-systolic left ventricular volume; LVID-d/s = left ventricular inner dimension at diastole/systole.

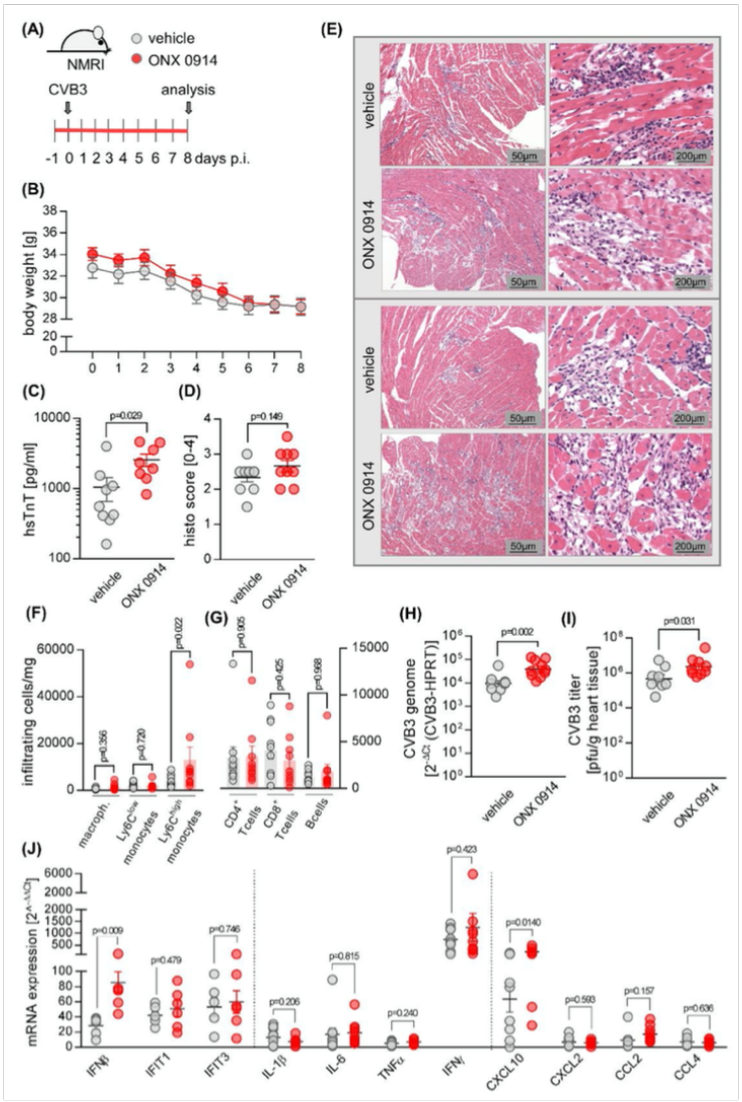

Figure 3. ONX 0914 treatment prior to infection with CVB3 exacerbates virus-mediated heart tissue injury. (**A**) Mice received either ONX 0914 (10 mg/kg bodyweight) or vehicle daily until day 8, starting one day prior to infection with 5×10^5 pfu of CVB3 strain 31-1-93. (**B**) Body weight was monitored daily and analyzed using two-way ANOVA. (**C**) On day 8, blood was drawn for measurement of hsTnT. (**D**) Mice were sacrificed on day 8. For histological analysis, HE-stained heart tissue sections were scored microscopically for myocardial cell death and inflammation. (**E**) Images from two representative mice per treatment group are shown. (**F**,**G**) Single cell solutions from heart tissue were generated and analyzed by flow cytometry for infiltration of immune cells. The viral load in infected mouse hearts was determined by quantification of the CVB3 genome, applying qPCR (**H**) and by quantification of viral titers, using plaque assay (**I**). Heart tissue was homogenized and RNA was extracted for qPCR-analysis of the indicated genes (**J**). Relative mRNA levels were normalized to the housekeeping gene HPRT and mRNA induction was normalized to data obtained with non-infected mice. Data are mean ± SEM, *p*-values are indicated in each graph. If not indicated otherwise, data was analyzed using unpaired *t*-test.

At the acute state of myocarditis, we found a reduced cardiac output in both treatment groups. Nevertheless, a closer investigation of the underlying aspects that might contribute to this lower cardiac output in infection illustrated different findings in the vehicle- and ONX 0914 groups. In the vehicle group, we observed a decrease of the left ventricular filling, which is indicative for a distributive failure of the vascular tone. Since the end-diastolic volume, reflecting left ventricular filling, was not altered by CVB3 infection in the ONX 0914 group, the treatment of NMRI mice with ONX 0914 apparently compensates for this vascular failure. On the other hand, we found a reduced left ventricular ejection fraction in this group. In line with the elevated myocardial cytotoxicity found in ONX 0914-treated mice, this might suggest systolic dysfunction as a potential effector of the reduced stroke volume. In vehicle-treated NMRI mice, we found no relevant decline of the ejection fraction at the acute state of myocarditis.

2.2. Influence of ONX 0914 on the Molecular Architecture of the 20S Proteasome Complex in Viral Myocarditis

Altogether, our data demonstrate that, at the acute stage of inflammation, ONX 0914 treatment promoted viral cytotoxicity, as reflected by cardiac myocyte damage, leading to elevated serum troponin T levels, and resultant inflammatory injury. In contrast to previous reports involving A/J mice [38], ONX 0914 had no relevant effect on systemic signs of viral infection, such as weight loss, cardiac output, or survival. Moreover, we found no evidence of impaired virus control in other tissues, such as spleen and pancreas (data not shown). Based on this controversial development of viral burden in different tissues, we questioned the inhibitory capacity of ONX 0914 with respect to the cardiac i-proteasome. The spleen, which shows no effect of ONX 0914 on the virus concentration (Figure S1, is a secondary lymphatic organ with important immune functions and the amount of i-proteasome expressed in naive spleen far outweighs that of the heart. These aspects make it an interesting organ to investigate the effects promoted by viral infection and ONX 0914 treatment on the catalytic subunits of the proteasome and to compare our results with those of heart tissue.

For both spleen (Figure 4) and heart tissue (Figure 5), representative mouse samples from vehicle- and ONX 0914-treated groups were analyzed separately, comparing uninfected controls (day 0) for each group to the early phase of infection (day 2) as well as acute (day 8) and chronic (day 28) stages of viral myocarditis. For mice treated with the vehicle, in murine splenic tissue, determination of mRNA levels for the catalytic i-proteasome subunits and their respective standard proteasome counterparts showed an increase of all i-proteasome subunits during acute myocarditis and a return to at least baseline values during chronic myocarditis (Figure 4A). Although temporal i-proteasome profiling was similar in ONX 0914-treated mice, the overall fold-induction was lower for all three i-proteasome subunits (Figure 4B). In cardiac tissue, we noted a similar mRNA expression profile for LMP2, LMP7, and MECL-1, yet with clear evidence of a much stronger induction of mRNA expression (Figure 5A,B), which is in line with pronounced inflammatory responses specifically in the heart during viral myocarditis. Throughout infection, mRNA profiles of standard proteasome subunits remained unchanged in both spleen and heart tissue, regardless of the treatment group.

We then performed Western blot analysis of the proteasome subunits. Corresponding to the respective mRNA profiles, in spleen we found slightly elevated expression levels of the i-proteasome subunits, revealing a mild reduction of the low abundance standard proteasome counterpart in vehicle-treated mice at day 8 post-infection (Figure 4C/E). ONX 0914 treatment had no relevant effects on i-proteasome induction and, other than in vehicle-treated animals, led to increased expression of the standard proteasome, particularly at day 8 post-infection (Figure 4D). To provide a direct comparison between treatment groups, a sample from one representative animal per group and day of infection was loaded onto the same gel (Figure 4E). Inhibition of a catalytic subunit by ONX 0914 is reflected by altered electrophoretic mobility due to an increased molecular weight, resulting in slower migration in SDS PAGE. Overall quantification of such alterations of molecular weight due to ONX 0914 treatment revealed an inhibition of all three i-proteasome subunits during the acute stage of infection in the spleen.

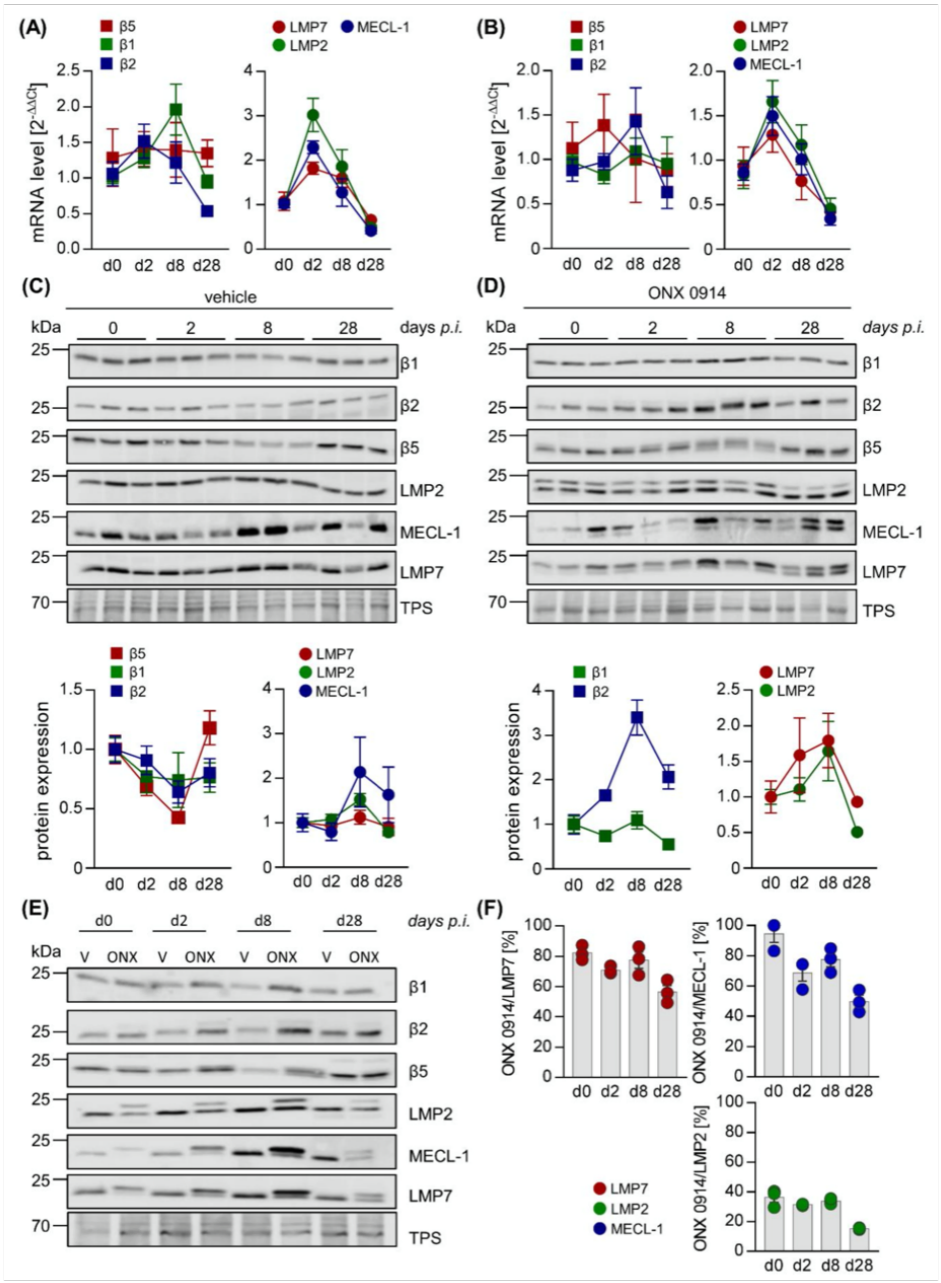

Figure 4. ONX 0914 selectively binds to i-proteasome subunits in the spleen during acute and chronic stages of viral myocarditis. Total RNA was extracted from spleen tissue of vehicle- (**A**) and ONX 0914- (**B**) treated mice sacrificed at different time points after CVB3 infection and mRNA expression levels were determined by qPCR for subunits β5, β1, and β2 (standard proteasome) as well as their i-proteasome counterparts LMP7, LMP2, and MECL-1, respectively. (**C**,**D**) Protein homogenates were obtained and subjected to Western blot analysis, showing the protein expression for the indicated

catalytic subunits of the proteasome complex for three different animals per group (vehicle: C; ONX 0914: D) on days 0, 2, 8, and 28 post-infection. Analysis of β5 and MECL-1 did not yield reliable densitometric readings and their protein expression is subsequently not shown. The section of the blot corresponding to 45 kDa treated with total protein stain indicates protein loading in each lane. Protein expression (mean ± SEM) was quantified using Image Studio Lite. Relative protein expression levels normalized to baseline controls and protein loading are shown. (**E**) To compare efficacy of i-proteasome inhibition at the different stages of infection, protein homogenates, obtained from a representative animal of each group (vehicle- and ONX 0914 treatment, days 0, 2, 8, and 28), were loaded onto the same SDS gel and Western blot analysis was performed as indicated. Total protein stain served as the loading control. (**F**) Covalent binding of ONX 0914 to the catalytic subunits of the proteasome induces an upward shift of the protein band for the respective proteasome subunit, indicative of an elevation of its molecular weight by the binding of ONX 0914. Based on the shifts detected with the Western blot analysis depicted in (**C**) and (**D**), the relative inhibition achieved by ONX 0914 was calculated for each i-proteasome subunit. This was accomplished through division of the signal from the upper (ONX 0914-bound) band by the total expression signal, which was calculated by the addition of both upper and lower bands in each individual lane.

ONX 0914 preferentially bound to LMP7 and MECL-1, revealing comparably lower proportional inhibition of LMP2. Long-term treatment of mice with ONX 0914 for 28 days decreased the proportion of ONX 0914-bound i-proteasome subunits in comparison to earlier stages of infection (Figure 4F), which might indicate a loss of efficacy for ONX 0914 over time.

As suggested by robust induction of i-proteasome mRNAs in heart tissue during acute infection, protein expression profiling confirmed the pronounced upregulation of the i-proteasome, peaking on day 8 at the acute stage in cardiac tissue and remaining elevated during the chronic stage on day 28, regardless of ONX 0914 treatment.

Standard proteasome expression was decreased to a comparable degree on day 8 (Figure 5C,D). Although ONX 0914 bound to all three i-proteasome subunits, showing a similar preference for LMP7 as seen in splenic tissue, we observed a drop in the efficacy of i-proteasome inhibition during the acute stage on day 8, coinciding with a loss of selectivity for the i-proteasome, particularly at this stage (Figure 5D–F). ONX 0914 also bound to the standard proteasome subunit β5, resulting in its partial inhibition prior to infection. Importantly, at the same time as i-proteasome formation and inhibition increased, we found a shift from partially towards completely inhibited β5 subunits on day 8 (Figure 5F).

Altogether, these data demonstrate that ONX 0914 incompletely inhibits the i-proteasome, formed in infected mouse hearts, and simultaneously affects the standard proteasome subunit β5 to a remarkable extent. Our data indicate a modified inhibitory capacity of ONX 0914 for proteasome subunits in non-immune cells, where the i-proteasome is strongly induced after infection and ONX 0914 shows lower selectivity for the i-proteasome.

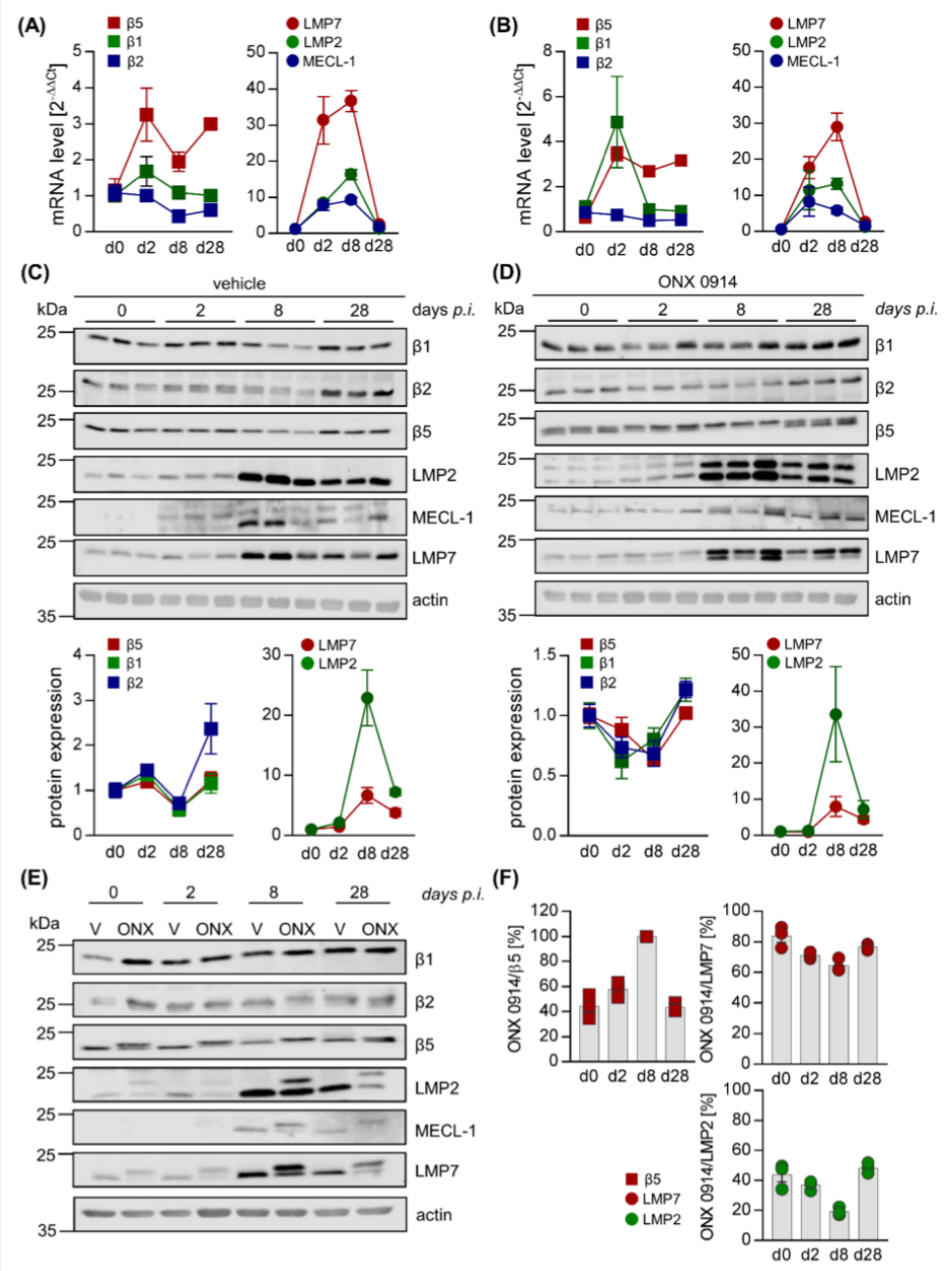

Figure 5. Loss of selectivity of ONX 0914 for the i-proteasome during acute viral myocarditis in heart tissue. Total mRNA was extracted from heart tissue of vehicle– (**A**) and ONX 0914– (**B**) treated mice sacrificed at different time points post CVB3 infection and expression levels were determined by qPCR for subunits β5, β1, and β2 (standard proteasome) as well as their i-proteasome counterparts LMP7, LMP2, and MECL-1, respectively. (**C**,**D**) Protein homogenates were obtained and subjected to Western blot analysis, showing the protein expression of the respective subunits for three different animals per

group (vehicle: C; ONX 0914: D) on days 0, 2, 8, and 28 post-infection for the indicated catalytic subunits of the proteasome complex. Actin indicates protein loading. Protein expression (mean ± SEM) was quantified using Image Studio Lite. Relative protein expression levels normalized to baseline controls and protein loading are shown. We were not able to quantify the protein expression levels for MECL-1. (**E**) To compare efficacy of i-proteasome inhibition at the different stages of infection, protein homogenates obtained from a representative animal for each group (vehicle- and ONX 0914 treatment, days 0, 2, 8, and 28) were loaded onto the same SDS gel and Western blot analysis was performed as indicated. Actin served as loading control. (**F**) Based on the shifts of the molecular weight of proteasome subunits detected by Western blot analysis (**C**,**D**), the relative inhibition achieved by ONX 0914 was calculated for each i-proteasome subunit, as well as for β5 of the standard proteasome (as described in Figure 4F).

3. Discussion

Based on the anti-inflammatory capacity accomplished by treating mice with i-proteasome-selective inhibitors, in this study we determined how ONX 0914, a broadly studied epoxyketone-based compound with irreversible inhibitory kinetics, affects virus-induced inflammation and remodeling processes, resulting in chronic myocarditis. Using the NMRI mouse model of CVB3 myocarditis, we found that ONX 0914, when given during the entire acute phase after infection, interfered with host processes needed to counteract virus-induced cytotoxicity and thereby mediated tissue injury, all resulting in severe inflammatory responses. Whereas ONX 0914 was specific for the i-proteasome in tissues, such as spleen, that constitutively have a high abundance of this isoform, the proportion of ONX 0914-bound i-proteasome subunits declined in the heart, when this proteasome isoform accumulated. In this phase, ONX 0914 bound completely to the cardiac standard proteasome subunit β5, which harbors the main chymotryptic-like activity of the proteasome.

The genetic background associated with the immunological make up of NMRI mice, although not well-characterized, is thought to predispose these mice to the development of a chronic course of viral myocarditis [37]. Progression towards chronic heart tissue injury in this strain is a consequence of acute myocarditis, which in A/J mice, showing a severe systemic inflammatory response after infection with cardiotropic CVB3 [44], is principally reversible by ONX 0914 [38]. Nevertheless, our data clearly demonstrate that the profound anti-inflammatory effects induced by ONX 0914, illustrated in the context of both viral infection [38,47] and autoimmunity [20,28,29,48], do not primarily affect the pathogenesis induced by viral infection in NMRI mice. In fact, we found that intact proteasome activity enables mice to cope better with the invading pathogen. The findings of this study echo our previous report on ONX 0914-mediated exacerbation of virus-triggered cardiac pathology in C57BL/6 mice [38] and is supported by the detection of a markedly increased fungal burden in a mouse model of *Candida albicans* infection [31]. For both pathogens, C57BL/6 mice were investigated and ONX 0914 inhibited the innate antiviral and antifungal immunity required for efficient control of these pathogens. The elevated pathogen load triggered the resulting recruitment of myeloid immune cells. Although the present study confirms elevated immunopathology in ONX 0914-treated mice to be most likely attributed to a higher concentration of the pathogen, our findings differ regarding the intact activation e.g., of IFN responses in NMRI mice. We have no experimental evidence, other than that previously reported in C57BL/6 mice [38,49], that ONX 0914 affects innate pathways of the IFN response, which could influence replication and spreading of the virus in NMRI mice as well. The IFN signature was similar in both vehicle- and ONX 0914-treated mice. In fact, corresponding to increased viral load at the acute state of myocarditis, IFN production was enhanced in the ONX 0914 group and this might be a result of the higher pathogen burden, a main determinant for the magnitude of such responses.

An alternative aspect that needs to be considered regarding the exacerbation of viral myocarditis in ONX 0914-treated NMRI mice, involves the initially proposed specific role of the i-proteasome in antigen presentation [15]. One could assume that i-proteasome inhibition impairs CD8 T cell immunity

and this determines the reported exacerbation in ONX 0914-treated mice. However, other than intracellular pathogens, such as LCMV [50] or *Listeria monocytogenes* [51], CVB3 infection elicits only a weak expansion of $CD8^+$ T effector cells [8,52,53]. Moreover, we demonstrated intact effector T and B cell responses, as well as unaffected memory responses, in both ONX 0914-treated and LMP7-deficient C57BL/6 mice after CVB3 infection [3,38]. Altogether, we conclude that alterations of the adaptive immune response, which might be mediated by ONX 0914 [30,54], are not among its main effectors, leading to exacerbated pathology in CVB3-infected NMRI mice. Quite in contrast to its pleiotropic cellular functions in the regulation of inflammatory signaling cascades and in antigen presentation in the host cell, the UPS can also be utilized to control the abundance of viral proteins in infected cells [25]. Direct interactions between viral and host-cell proteins [55] may offer a putative explanation for how inhibition of the proteasome complex, as shown here for ONX 0914 treatment in NMRI mice, might affect the viral load independent of the innate and adaptive immune responses. Molecular aspects, shedding light onto the connection between the expression of viral proteins and their degradation by the proteasome, are known for enterovirus 71 (EV71), another member of the Picornaviridae family. In wild-type EV71, sumoylation, a post-translational ubiquitin-like protein modification, of the viral protease 3C directs this viral protein to the ubiquitination apparatus, marking it for degradation by the proteasome and correlating with lower virus production. Clinically relevant EV71 strains with enhanced virulence, however, lack the sumoylation site of the viral protease 3C, thereby increasing virus protein stability and promoting viral replication [56]. This exemplary mechanistic illustration of viral and host-cell protein interaction elegantly demonstrates how viral replication may be facilitated, whenever degradation of viral proteins by the proteasome is inhibited. The latter can be considered as part of the cellular defense against invading pathogens and inhibition of proteasome activity, as shown here for ONX 0914, might thereby also promote viral replication.

Death of cardiomyocytes by increased viral cytotoxicity during the acute phase of myocarditis in ONX 0914-treated NMRI mice is reflected by higher release of TnT and the cellular injury in the heart triggers an elevated infiltration of inflammatory monocytes, compared to the vehicle group. This adverse inflammatory response is in contrast to our previous demonstration of ONX 0914-mediated reversal of immunopathology in A/J mice. Here, ONX 0914 blocks the detrimental cytokine overproduction, reminiscent of sepsis, and thereby protects from viral pathology and infiltration of myeloid immune cells into the heart [38]. Interestingly, although in NMRI mice the ONX 0914-mediated anti-inflammatory effects are overwhelmed by elevated viral cytotoxicity, a closer assessment of cardiac function indeed confirms some protective properties of ONX 0914 in NMRI mice as well. The decreased end-diastolic volume mice have during the acute state of myocarditis reflects the vascular dilatation mediated by pro-inflammatory molecules within the systemic inflammatory response syndrome. Similar to A/J mice, ONX 0914 reduces this drop of left ventricular filling during infection and thereby partially compensates for the reduced cardiac output during viral myocarditis. Despite preserved ventricular filling, the cardiac output is also reduced in myocarditis in the ONX 0914 group and this is mostly attributed to elevated viral cytotoxicity.

Another aspect, how particularly unselective proteasome inhibitors might affect cardiac function, involves the central role of the proteasome complex for the timely degradation of sarcomeric proteins, the main components for contractile function of cardiomyocytes. Therefore, we also need to consider the selectivity of ONX 0914, an irreversible inhibitor of the i-proteasome [20], for the cardiac proteasome complex. In naive splenic tissue, with a high abundance of residential immune cells and likewise a high constitutive level of i-proteasome expression, ONX 0914 specifically inhibited the i-proteasome, yet over time the efficacy of the respective binding to the i-proteasome declined. Moreover, prolonged ONX 0914 treatment might also result in a shift from i-proteasome selectivity towards elevated inhibition of the standard proteasome as shown here for heart tissue and as previously suggested by others [22]. In fact, since ONX 0914, a covalently reacting and irreversible LMP7 inhibitor, reacts to some degree with β5 [20], it was expected to show diminishing isoform selectivity over time [22]. Our observation, suggesting that de novo formed i-proteasomes are less efficiently inhibited by ONX 0914 over time, might have

clinical implications, whenever long-term treatment may be required. In such cases, putative side effects might arise from disturbed proteostasis [10,11], leading not only to the death of immune [57], but also of non-immune cells. Recently, the Nathan group proposed a way to circumvent the issue observed here by introducing N,C-capped dipeptidomimetics, showing a much higher selectivity for LMP7 over β5 [58] than that accomplished by ONX 0914 [20]. Stable selectivity of dipeptidomimetic i-proteasome inhibitors was shown in in vitro studies, however, data on subunit selectivity are not yet available for in vivo experiments. In any case, we see the advantages potentially achievable by irreversible i-proteasome selective inhibitors, since a loss of i-proteasome subunit selectivity and the resulting inhibition of the standard proteasome, as shown here for repetitive treatment with ONX 0914 in the heart, can perturb protein homeostasis, e.g., in tissues with highly abundant standard proteasome expression levels.

Achievement of partially overlapping inhibition of the standard proteasome subunit β5 by ONX 0914 in cardiac tissue, as shown here, relates back to the observed cardiotoxicity, induced by marketed proteasome inhibitors for the treatment of multiple myeloma [59,60] by their inhibition of the cardiac proteasome complex. Like other cells, cardiomyocytes depend on cellular responses for the timely removal of misfolded proteins and this is orchestrated in part by the UPS. Carfilzomib, a proteasome inhibitor used in the clinics, mainly targets the β5/β5i subunits and causes cardiomyocyte toxicity, most likely through proteotoxic stress resulting from the inhibition of standard proteasome-dependent sarcomeric protein turnover, with subsequent activation of the unfolded protein response and apoptosis [61]. Accumulating dysfunctional sarcomeric proteins can perturb the functional integrity of the sarcomere, required for the contractile function of the heart. Hence, defective activity of the cardiac proteasome, as gradually accomplished by ONX 0914 in acute myocarditis of NMRI mice, might have detrimental effects on cardiomyocyte function. In addition to elevated viral cytotoxicity, the cumulative inhibition of the standard proteasome by an irreversible immunoproteasome inhibitor with general binding capacity for β5 presents a risk of toxicity [13] and might partially explain why NMRI mice showed impaired systolic function upon treatment with ONX 0914, assuming a parallel between this treatment and the effect accomplished by licensed proteasome inhibitors.

4. Materials and Methods

4.1. Mouse Studies

Outbred NMRI mice were purchased from Charles River, Germany and kept in the animal facility at Charité University Medical Center, Berlin. Myocarditis was induced in 6-week old male mice by intraperitoneal infection with 5×10^5 plaque forming units (pfu) CVB3 31-1-93 [45]. For the therapeutic i-proteasome inhibitor treatment, mice were injected subcutaneously with 5–10 mg/kg bodyweight (BW) ONX 0914 or the vehicle Captisol daily from day 3 to 8 (acute viral myocarditis). For experiments investigating chronic viral myocarditis, treatments were continued three times per week until day 28. For the prophylactic approach, the general treatment plan remained the same, but injections were instead given starting one day prior to infection. On the final day of each experiment, after echocardiography, organs were collected for further analysis and immediately frozen in liquid nitrogen. Organs were stored at −80 °C. Whole blood was centrifuged at 4 °C and 10,000 rcf for 15 min to separate serum, which was then collected and stored at −80 °C. All animal experiments were in accordance with the local regulations and guidelines as well as approved by the Committee on the Ethics of Animal Experiments of Berlin state authorities (TVA Nr. G103/18 and G0274/13). All efforts were made to minimize suffering.

4.2. Echocardiography

Transthoracic echocardiography was performed on a VisualSonics Vevo770 High-Frequency imaging system (FUJIFILM VisualSonics, Toronto, ON, Canada) using a high-resolution scan head CRMV-707B; 15-45Hz). Mice were anaesthetized with 1–2.5% isoflurane and fixed on a heated pad with integrated electrodes for continuous ECG measurement. An experienced technician, who was not aware of treatment allocation, performed all measurements. Standard planes and measurements were

obtained using standard M-mode. Functional and dimensional calculations are based on the parasternal long axis view of the left ventricle.

4.3. Proteasome Inhibitor ONX 0914

For subcutaneous administration, ONX 0914 (Cayman Chemicals, Ann Arbor, US.A.) was dissolved at a concentration of 1–2 mg/mL in an aqueous solution of 1 mg/mL Captisol (Ligand Pharmaceuticals, San Diego, CA; USA.) and sodium citrate at pH 3.5. Aliquots of both ONX 0914 and Captisol were stored at −20 °C.

4.4. Quantification of Infectious Viral Particles

Organ virus titers were determined by standard plaque assay on HeLa cells grown in monolayers. Experiments were performed in duplicates on 24-well cell culture plates using 10-fold titrations of homogenized organs to infect cells for 30 min at 37 °C. Supernatant was carefully discarded before applying agar overlays (containing MEM, 1% penicillin/streptomycin, 2.3 g/L $NaHCO_3$, 9.2% FBS and 0.7% Difco Agar Noble (BD Bioscience, Heidelberg, Germany)). After incubation for 48 h, cells were stained with MTT (3-(4,5-dimethylthiazol-2-yl)-2,5-diphenyl tetrazolium bromide), incubated for at least 1 h and plaques were subsequently counted.

4.5. Histology

All histological samples were fixed in 4% formaldehyde overnight before analysis. As previously described, 5 µm thick slices of heart tissue were stained with hematoxylin/eosin and Masson's trichrome [45].

4.6. Flow Cytometry

To generate samples for flow cytometry, hearts were flushed with 10 mL PBS before removal and washed again in PBS before a piece for FACS analysis was weighed and stored in washing buffer (RPMI 1640 with 2% FBS, 1% penicillin/streptomycin, and 30 mM HEPES). Cells were extracted by digestion using 1.0 mg/mL collagenase type 2 (Worthington Biochemical Corporation, Lakewood, NJ, USA) and 0.15 mg/mL DNase I (Sigma-Aldrich, St. Louis, MO, USA.) for 30 min at 37 °C under continuous agitation. EDTA was added at a concentration of 10 mM before samples were processed through a 70 µm cell strainer. Erythrocyte lysis was performed for 3–5 min at room temperature using 10 mM $KHCO_3$, 155 mM NH_4Cl, and 0.1 mM EDTA. Cells corresponding to 20 mg heart tissue were incubated with Fc blocking reagent (Miltenyi) at a concentration of 1:50 for 15 min at 4 °C. Cells were then stained with the antibodies listed below for 15 min at 4 °C. Samples were washed with FACS buffer (PBS with 2% FBS and 2 mM EDTA) and PBS before Fixable Viability Dye eFluor 780 (eBioscience, San Diego, CA, USA.) was applied according to manufacturer's instructions. Samples were fixed using 2% formaldehyde in PBS for 30 min at room temperature and washed with PBS prior to addition of 123count eBeads (eBioscience) for the quantification of total cell numbers. Antibodies were purchased from BD (CD69 clone H1.2F3, CD4 clone RM4-5, CD8α clone 53-6.7, CD45 clone 30-F11, B220 clone RA3-6B2, CD3 clone 145-2C11), Biolegend (San Diego, CA, USA.) (F4/80 clone BM8, CD11b clone M1/70, Ly6G clone 1A8, CD11c clone N418, Ly6C clone HK1.4) or eBioscience (CD49b clone DX5). Flow-cytometric analysis was conducted on a BD FACSymphony flow cytometer and data were analyzed using FlowJo V10 software (Ashland, Wilmington, DE, USA), applying the gating strategy depicted in Figure S2.

4.7. RNA Isolation, cDNA Synthesis, and qPCR

For RNA isolation, Trizol Reagent (ThermoFisherScientific, Waltham, MA, USA) was used according to the manufacturer's instructions. Samples were incubated with 0.1 U/µL DNAseI (ThermoFisherScientific, Waltham, WA, USA) prior to cDNA synthesis using random hexamer primers and MLV-reverse transcriptase (Promega, Madison, WI, USA). Using TaqMan Fast Universal PCR

Master Mix (ThermoFisherScientific, Waltham, MA, USA) as well as primers and probes of TaqMan gene expression assays (ThermoFisherScientific, Waltham, MA, USA), qPCR was performed on a StepOnePlus real-time PCR System ((ThermoFisherScientific, Waltham, MA, USA). CVB3 sequences for primer/probe-combinations used were 5′-CCCTGAATGCGGCTAATCC-3′ (sense), 5′-ATTGTCAC CATAAGCAGCCA-3′ (anti-sense) for the primers and 5′-FAM-TGCAGCGGAACCG- MGB-3′ for the probe. The housekeeping control employed was mHPRT, with the sequences 5′-ATCATTATGCC GAGGATTTGGAA-3′ (sense), 5′-ATTGTCACCATAAGCAGCCA-3′ (anti-sense) for the primers and 5′-FAM-TGGACAGGACTGAAAGACTTGCTCGAGATG-MGB-3′ for the probe.

4.8. Western Blot Analysis

Tissue samples were homogenized in lysis buffer containing 50 mM Tris-HCl (pH 8.0), 150 mM NaCl, 1% NP40, 1 mM EDTA, 0.1% SDS, 0.5% Na-deoxycholate, 1 × cOmplete protease inhibitor cocktail (Sigma-Aldrich, St. Louis, MO, USA) and 5 µM NEM. Bradford assays were performed to determine protein concentrations (measured on a Synergy HT plate reader (BIO-TEK, Winooski, VT, USA) before samples were diluted to 1 µg/µL in Laemmli buffer. For gel electrophoresis, samples were applied to a 12% acrylamide-bisacrylamide gel and run in an Mini PROTEAN Tetra system (BioRAD, Hercules, CA, USA) before tank blotting was performed using the same system. The following primary antibodies were used for immunostaining: β1 (K43, lab stock), β2 (Abcam, Cambridge, UK), β5 (Abcam, Cambridge, UK), LMP2 (Abcam, Cambridge, UK), MECL-1 (K65, lab stock), LMP7 (K63, lab stock), β-actin (C4, Merck Millipore, Burlington, VT, USA). Secondary IRD680CW or IRDye800CW labeled antibodies (Li-Cor Biosciences, Lincoln, MA, USA) were used for the detection on an Odyssey CLx imager (Li-Cor Bioscience, Lincoln, MA, USA). To control for equal loading of spleen tissue lysates, REVERT®Total Protein stain (Li-Cor Bioscience, Lincoln, MA, USA) was performed according to manufacturer's instructions. Protein bands were quantified using ImageStudio Light 5.2 (Li-Cor Bioscience, Lincoln, MA, USA) and were normalized to either β-actin or total protein stain. Some blots had a poor signal-to-noise ratio and densitometric analysis was not possible.

4.9. Statistics

Data was analyzed using GraphPad Prism 7.0 (GraphPad Software, San Diego, CA, USA). Logarithmic data such as virus titers was transformed logarithmically before data was plotted and statistically analyzed. All data was tested for normal distribution using the D'Agostino-Pearson normality test. For normally distributed data, paired or unpaired *t*-tests were performed. Non-normally distributed data were analyzed using either Wilcoxon-signed rank test or Mann–Whitney test. To compare treatment groups or time points, repeated measurements two-way ANOVA with Sidak's multiple comparisons were performed. Data is displayed as mean ± SEM unless otherwise indicated.

Supplementary Materials: The following are available online at http://www.mdpi.com/2073-4409/9/5/1093/s1, Figure S1. Influence of ONX 0914 on the inflammatory response in spleen after CVB3 infection. Figure S2: Gating strategy for flow cytometric analysis of heart tissue.

Author Contributions: Conceptualization, A.B.; Methodology, H.L.N., K.K., Z.K., A.H., M.K. and A.B.; Validation, H.L.N., S.H.; Formal analysis, H.L.N., S.H., K.K., Z.K. and A.H.; Investigation, H.L.N., S.H., K.K.; Resources, A.B.; Data curation, H.L.N. and S.H.; Writing—Original draft preparation, H.L.N. and A.B.; Writing—Review and editing, A.B.; Visualization, H.L.N., S.H., A.B.; Supervision, A.B.; Project administration, A.B; Funding acquisition, A.B., Z.K. All authors have read and agreed to the published version of the manuscript.

Funding: The German Research Foundation funded this research: BE 6335/4-1, BE 6335/4-3 and BE 6335/6-1, CRC1292 project 02 to A.B. and K.A. 1797/7-1 and K.A. 1797/7-3 to Z.K. AB receives support from the Foundation for Experimental Biomedicine Zurich, Switzerland. H.L.N. was supported by a M.D. scholarship provided by the Berlin Institute of Health. M.K. receives support from the International Max-Planck-Research-School for Infectious Diseases and Immunology (IMPRS-IDI), Berlin.

Acknowledgments: We acknowledge administrative and technical support by Anika Lindner, Karolin Voss, Sandra Bundschuh, and Martin Taube. We acknowledge Sandra Pinkert and Carl Christoph Goetzke for methodological advice. We acknowledge Toralf Kaiser and the support provided by the flow cytometry core facility of the DRFZ, Berlin, Germany. We also thank E. Wade for critical reading of the manuscript and helpful comments.

Conflicts of Interest: The authors declare no conflict of interest. The funders had no role in the design of the study; in the collection, analyses, or interpretation of data; in the writing of the manuscript, or in the decision to publish the results.

Abbreviations

bpm	beats per minute
CCL2	chemokine ligand 2
CCL4	chemokine ligand 4
CVB3	coxsackievirus B3
CXCL2	C-X-C- motif chemokine ligand 2
CXCL10	C-X-C- motif chemokine ligand 10
DAMP	damage-associated molecular pattern
EF	ejection fraction
HE	hematoxylin-eosin
IL	interleukin
IFIT1/3	interferon-induced protein with tetratricopeptide repeats 1/3
IFN	interferon
i-proteasome	immunoproteasome
LMP2	low molecular weight protein 2
LMP7	low molecular weight protein 7
LVID-d/-s	left ventricular inner dimension at diastole/systole
LCMV	lymphocytic choriomeningitis virus
MHC	major histocompatibility complex
mHPRT	mouse hypoxanthine-guanine phosphoribosyl transferase
MECL-1	multicatalytic endopeptidase complex-like 1
PAMP	pathogen-associated molecular pattern
PW-Doppler	pulsed-wave Doppler
(hs)TnT	(high sensitive) troponin T
UPS	ubiquitin-proteasome system
vol d/s	end-diastolic/end-systolic volume

References

1. Dikic, I. Proteasomal and Autophagic Degradation Systems. *Annu. Rev. Biochem.* **2017**, *86*, 193–224. [CrossRef] [PubMed]
2. Goldberg, A.L. Protein degradation and protection against misfolded or damaged proteins. *Nature* **2003**, *426*, 895–899. [CrossRef] [PubMed]
3. Opitz, E.; Koch, A.; Klingel, K.; Schmidt, F.; Prokop, S.; Rahnefeld, A.; Sauter, M.; Heppner, F.L.; Völker, U.; Kandolf, R.; et al. Impairment of immunoproteasome function by beta5i/LMP7 subunit deficiency results in severe enterovirus myocarditis. *PLoS Pathog.* **2011**, *7*, 1–13. [CrossRef] [PubMed]
4. Gaczynska, M.; Rock, K.L.; Goldberg, A.L. Gamma-Interferon and Expression of Mhc Genes Regulate Peptide Hydrolysis by Proteasomes. *Nature* **1993**, *365*, 264–267. [CrossRef] [PubMed]
5. Spur, E.-M.; Althof, N.; Respondek, D.; Klingel, K.; Heuser, A.; Overkleeft, H.S.; Voigt, A.; Beling, A. Inhibition of chymotryptic-like standard proteasome activity exacerbates doxorubicin-induced cytotoxicity in primary cardiomyocytes. *Toxicology* **2016**, *353*, 34–47. [CrossRef]
6. Pickering, A.M.; Koop, A.L.; Teoh, C.Y.; Ermak, G.; Grune, T.; Davies, K.J. The immunoproteasome, the 20S proteasome and the PA28 alpha beta proteasome regulator are oxidative-stress-adaptive proteolytic complexes. *Biochem. J.* **2010**, *432*, 585–594. [CrossRef]
7. Aki, M.; Shimbara, N.; Takashina, M.; Akiyama, K.; Kagawa, S.; Tamura, T.; Tanahashi, N.; Yoshimura, T.; Tanaka, K.; Ichihara, A. Interferon-γ Induces Different Subunit Organizations and Functional Diversity of Proteasomes. *J. Biochem.* **1994**, *115*, 257–269. [CrossRef]
8. Jäkel, S.; Kuckelkorn, U.; Szalay, G.; Plötz, M.; Textoris-Taube, K.; Opitz, E.; Klingel, K.; Stevanovic, S.; Kandolf, R.; Kotsch, K.; et al. Differential Interferon Responses Enhance Viral Epitope Generation by Myocardial Immunoproteasomes in Murine Enterovirus Myocarditis. *Am. J. Pathol.* **2009**, *175*, 510–518. [CrossRef]

9. Mishto, M.; Liepe, J.; Textoris-Taube, K.; Keller, C.; Henklein, P.; Weberruß, M.; Dahlmann, B.; Enenkel, C.; Voigt, A.; Kuckelkorn, U.; et al. Proteasome isoforms exhibit only quantitative differences in cleavage and epitope generation. *Eur. J. Immunol.* **2014**, *44*, 3508–3521. [CrossRef]
10. Ebstein, F.; Voigt, A.; Lange, N.; Warnatsch, A.; Schröter, F.; Prozorovski, T.; Kuckelkorn, U.; Aktas, O.; Seifert, U.; Kloetzel, P.-M.; et al. Immunoproteasomes are important for proteostasis in immune responses. *Cell* **2013**, *152*, 935–937. [CrossRef]
11. Seifert, U.; Bialy, L.; Ebstein, F.; Bech-Otschir, D.; Voigt, A.; Schröter, F.; Prozorovski, T.; Lange, N.; Steffen, J.; Rieger, M.; et al. Immunoproteasomes Preserve Protein Homeostasis upon Interferon-Induced Oxidative Stress. *Cell* **2010**, *142*, 613–624. [CrossRef]
12. Huber, E.M.; Basler, M.; Schwab, R.; Heinemeyer, W.; Kirk, C.J.; Groettrup, M.; Groll, M. Immuno- and Constitutive Proteasome Crystal Structures Reveal Differences in Substrate and Inhibitor Specificity. *Cell* **2012**, *148*, 727–738. [CrossRef] [PubMed]
13. Santos, R.D.L.A.; Bai, L.; Singh, P.K.; Murakami, N.; Fan, H.; Zhan, W.; Zhu, Y.; Jiang, X.; Zhang, K.; Assker, J.P.; et al. Structure of human immunoproteasome with a reversible and noncompetitive inhibitor that selectively inhibits activated lymphocytes. *Nat. Commun.* **2017**, *8*, 1692. [CrossRef] [PubMed]
14. Gaczynska, M.; Rock, K.L.; Spies, T.; Goldberg, A.L. Peptidase activities of proteasomes are differentially regulated by the major histocompatibility complex-encoded genes for LMP2 and LMP. *Proc. Natl. Acad. Sci. USA* **1994**, *91*, 9213–9217. [CrossRef] [PubMed]
15. Kincaid, E.Z.; Che, J.W.; York, I.; Escobar, H.; Reyes-Vargas, E.; Delgado, J.C.; Welsh, R.M.; Karow, M.L.; Murphy, A.J.; Valenzuela, D.M.; et al. Mice completely lacking immunoproteasomes show major changes in antigen presentation. *Nat. Immunol.* **2011**, *13*, 129–135. [CrossRef] [PubMed]
16. Tu, L.; Moriya, C.; Imai, T.; Ishida, H.; Tetsutani, K.; Duan, X.; Murata, S.; Tanaka, K.; Shimokawa, C.; Hisaeda, H.; et al. Critical role for the immunoproteasome subunit LMP7 in the resistance of mice to Toxoplasma gondii infection. *Eur. J. Immunol.* **2009**, *39*, 3385–3394. [CrossRef] [PubMed]
17. Chen, W.; Norbury, C.C.; Cho, Y.; Yewdell, J.W.; Bennink, J.R. Immunoproteasomes Shape Immunodominance Hierarchies of Antiviral $Cd8^+$ T Cells at the Levels of T Cell Repertoire and Presentation of Viral Antigens. *J. Exp. Med.* **2001**, *193*, 1319–1326. [CrossRef] [PubMed]
18. Nussbaum, A.K.; Rodriguez-Carreno, M.P.; Benning, N.; Botten, J.; Whitton, J.L. Immunoproteasome-deficient mice mount largely normal $CD8^+$ T cell responses to lymphocytic choriomeningitis virus infection and DNA vaccination. *J. Immunol.* **2005**, *175*, 1153–1160. [CrossRef]
19. Fehling, H.; Swat, W.; LaPlace, C.; Kühn, R.; Rajewsky, K.; Müller, U.; Von Boehmer, H. MHC class I expression in mice lacking the proteasome subunit LMP. *Science* **1994**, *265*, 1234–1237. [CrossRef]
20. Muchamuel, T.; Basler, M.; Aujay, M.A.; Suzuki, E.; Kalim, K.W.; Lauer, C.; Sylvain, C.; Ring, E.R.; Shields, J.; Jiang, J.; et al. A selective inhibitor of the immunoproteasome subunit LMP7 blocks cytokine production and attenuates progression of experimental arthritis. *Nat. Med.* **2009**, *15*, 781–787. [CrossRef]
21. Basler, M.; Lindstrom, M.M.; LaStant, J.J.; Bradshaw, J.M.; Owens, T.D.; Schmidt, C.; Maurits, E.; Tsu, C.; Overkleeft, H.S.; Kirk, C.J.; et al. Co-inhibition of immunoproteasome subunits LMP2 and LMP7 is required to block autoimmunity. *EMBO Rep.* **2018**, *19*, e46512. [CrossRef] [PubMed]
22. Karreci, E.S.; Fan, H.; Uehara, M.; Mihali, A.B.; Singh, P.K.; Kurdi, A.T.; Solhjou, Z.; Riella, L.V.; Ghobrial, I.; Laragione, T.; et al. Brief treatment with a highly selective immunoproteasome inhibitor promotes long-term cardiac allograft acceptance in mice. *Proc. Natl. Acad. Sci. USA* **2016**, *113*, E8425–E8432. [CrossRef] [PubMed]
23. Basler, M.; Li, J.; Groettrup, M. On the role of the immunoproteasome in transplant rejection. *Immunogenetics* **2018**, *71*, 263–271. [CrossRef] [PubMed]
24. Kisselev, A.F.; Groettrup, M. Subunit specific inhibitors of proteasomes and their potential for immunomodulation. *Curr. Opin. Chem. Boil.* **2014**, *23*, 16–22. [CrossRef]
25. Beling, A.; Kespohl, M. Proteasomal Protein Degradation: Adaptation of Cellular Proteolysis with Impact on Virus—And Cytokine-Mediated Damage of Heart Tissue During Myocarditis. *Front. Immunol.* **2018**, *9*. [CrossRef]
26. Koerner, J.; Brunner, T.; Groettrup, M. Inhibition and deficiency of the immunoproteasome subunit LMP7 suppress the development and progression of colorectal carcinoma in mice. *Oncotarget* **2017**, *8*, 50873–50888. [CrossRef]

27. Vachharajani, N.; Joeris, T.; Luu, M.; Hartmann, S.; Pautz, S.; Jenike, E.; Pantazis, G.; Prinz, I.; Hofer, M.J.; Steinhoff, U.; et al. Prevention of colitis-associated cancer by selective targeting of immunoproteasome subunit LMP. *Oncotarget* **2017**, *8*, 50447–50459. [CrossRef]
28. Bockstahler, M.; Fischer, A.; Goetzke, C.C.; Neumaier, H.L.; Sauter, M.; Kespohl, M.; Müller, A.-M.; Meckes, C.; Salbach, C.; Schenk, M.; et al. Heart-Specific Immune Responses in an Animal Model of AutoimmuneRelated Myocarditis Mitigated by an Immunoproteasome Inhibitor and Genetic Ablation. *Circulation* **2020**. [CrossRef]
29. Basler, M.; Mundt, S.; Muchamuel, T.; Moll, C.; Jiang, J.; Groettrup, M.; Kirk, C.J. Inhibition of the immunoproteasome ameliorates experimental autoimmune encephalomyelitis. *EMBO Mol. Med.* **2014**, *6*, 226–238. [CrossRef]
30. Li, J.; Koerner, J.; Basler, M.; Brunner, T.; Kirk, C.J.; Groettrup, M. Immunoproteasome inhibition induces plasma cell apoptosis and preserves kidney allografts by activating the unfolded protein response and suppressing plasma cell survival factors. *Kidney Int.* **2019**, *95*, 611–623. [CrossRef]
31. Mundt, S.; Basler, M.; Buerger, S.; Engler, H.; Groettrup, M. Inhibiting the immunoproteasome exacerbates the pathogenesis of systemic Candida albicans infection in mice. *Sci. Rep.* **2016**, *6*, 19434. [CrossRef] [PubMed]
32. Ersching, J.; Vasconcelos, J.R.; Ferreira, C.P.; Caetano, B.C.; Machado, A.V.; Bruna–Romero, O.; Baron, M.A.; Ferreira, L.R.P.; Cunha-Neto, E.; Rock, K.L.; et al. The Combined Deficiency of Immunoproteasome Subunits Affects Both the Magnitude and Quality of Pathogen- and Genetic Vaccination-Induced CD8+ T Cell Responses to the Human Protozoan Parasite Trypanosoma cruzi. *PLOS Pathog.* **2016**, *12*, e1005593. [CrossRef] [PubMed]
33. Corsten, M.F.; Schroen, B.; Heymans, S. Inflammation in viral myocarditis: Friend or foe? *Trends Mol. Med.* **2012**, *18*, 426–437. [CrossRef] [PubMed]
34. Kallewaard, N.L.; Zhang, L.; Chen, J.-W.; Guttenberg, M.; Sánchez, M.D.; Bergelson, J.M. Tissue-Specific Deletion of the Coxsackievirus and Adenovirus Receptor Protects Mice from Virus-Induced Pancreatitis and Myocarditis. *Cell Host Microbe* **2009**, *6*, 91–98. [CrossRef] [PubMed]
35. Klingel, K.; Hohenadl, C.; Canu, A.; Albrecht, M.; Seemann, M.; Mall, G.; Kandolf, R. Ongoing enterovirus-induced myocarditis is associated with persistent heart muscle infection: Quantitative analysis of virus replication, tissue damage, and inflammation. *Proc. Natl. Acad. Sci. USA* **1992**, *89*, 314–318. [CrossRef] [PubMed]
36. Szalay, G.; Meiners, S.; Voigt, A.; Lauber, J.; Spieth, C.; Speer, N.; Sauter, M.; Kuckelkorn, U.; Zell, A.; Klingel, K.; et al. Ongoing Coxsackievirus Myocarditis Is Associated with Increased Formation and Activity of Myocardial Immunoproteasomes. *Am. J. Pathol.* **2006**, *168*, 1542–1552. [CrossRef]
37. Pinkert, S.; Dieringer, B.; Klopfleisch, R.; Savvatis, K.; Van Linthout, S.; Pryshliak, M.; Tschöpe, C.; Klingel, K.; Kurreck, J.; Beling, A.; et al. Early Treatment of Coxsackievirus B3-Infected Animals with Soluble Coxsackievirus-Adenovirus Receptor Inhibits Development of Chronic Coxsackievirus B3 Cardiomyopathy. *Circ. Hearth Fail.* **2019**, *12*, e005250. [CrossRef]
38. Althof, N.; Goetzke, C.C.; Kespohl, M.; Voss, K.; Heuser, A.; Pinkert, S.; Kaya, Z.; Klingel, K.; Beling, A. The immunoproteasome-specific inhibitor ONX 0914 reverses susceptibility to acute viral myocarditis. *EMBO Mol. Med.* **2018**, *10*, 200–218. [CrossRef]
39. McCarthy, M.K.; Malitz, D.H.; Molloy, C.T.; Procario, M.C.; Greiner, K.E.; Zhang, L.; Wang, P.; Day, S.M.; Powell, S.R.; Weinberg, J.B. Interferon-Dependent Immunoproteasome Activity During Mouse Adenovirus Type 1 Infection. *Virology* **2016**, *498*, 57–68. [CrossRef]
40. Voigt, A.; Rahnefeld, A.; Kloetzel, P.M.P.; Krueger, E. Cytokine-induced oxidative stress in cardiac inflammation and heart failure—How the ubiquitin proteasome system targets this vicious cycle. *Front. Physiol.* **2013**, *4*, 42. [CrossRef]
41. Paeschke, A.; Possehl, A.; Klingel, K.; Voss, M.; Voss, K.; Kespohl, M.; Sauter, M.; Overkleeft, H.S.; Althof, N.; Garlanda, C.; et al. The immunoproteasome controls the availability of the cardioprotective pattern recognition molecule Pentraxin. *Eur. J. Immunol.* **2015**, *46*, 619–633. [CrossRef] [PubMed]
42. Epelman, S.; Liu, P.P.; Mann, D.L. Role of innate and adaptive immune mechanisms in cardiac injury and repair. *Nat. Rev. Immunol.* **2015**, *15*, 117–129. [CrossRef] [PubMed]
43. Gangaplara, A.; Massilamany, C.; Brown, D.M.; Delhon, G.; Pattnaik, A.K.; Chapman, N.; Rose, N.; Steffen, D.; Reddy, J. Coxsackievirus B3 infection leads to the generation of cardiac myosin heavy chain-α-reactive CD4 T cells in A/J mice. *Clin. Immunol.* **2012**, *144*, 237–249. [CrossRef] [PubMed]
44. Chow, L.H.; Gauntt, C.J.; McManus, B.M. Differential effects of myocarditic variants of Coxsackievirus B3 in inbred mice. A pathologic characterization of heart tissue damage. *Lab. Investig.* **1991**, *64*, 55–64. [PubMed]

45. Merkle, I.; Tonew, M.; Glück, B.; Schmidtke, M.; Egerer, R.; Stelzner, A. Coxsackievirus B3-induced chronic myocarditis in outbred NMRI mice. *J. Hum. Virol.* **2000**, *2*, 369–379.
46. Pappritz, K.; Savvatis, K.; Miteva, K.; Kerim, B.; Dong, F.; Fechner, H.; Muller, I.; Brandt, C.; López, B.; González, A.; et al. Immunomodulation by adoptive regulatory T-cell transfer improves Coxsackievirus B3-induced myocarditis. *FASEB J.* **2018**, *32*, 6066–6078. [CrossRef]
47. Mundt, S.; Engelhardt, B.; Kirk, C.J.; Groettrup, M.; Basler, M. Inhibition and deficiency of the immunoproteasome subunit LMP7 attenuates LCMV-induced meningitis. *Eur. J. Immunol.* **2015**, *46*, 104–113. [CrossRef]
48. Basler, M.; Dajee, M.; Moll, C.; Groettrup, M.; Kirk, C.J. Prevention of Experimental Colitis by a Selective Inhibitor of the Immunoproteasome. *J. Immunol.* **2010**, *185*, 634–641. [CrossRef]
49. Ichikawa, H.T.; Conley, T.; Muchamuel, T.; Jiang, J.; Lee, S.; Owen, T.; Barnard, J.; Nevarez, S.; Goldman, B.I.; Kirk, C.J.; et al. Beneficial effect of novel proteasome inhibitors in murine lupus via dual inhibition of type I interferon and autoantibody-secreting cells. *Arthr. Rheum.* **2012**, *64*, 493–503. [CrossRef]
50. Schwarz, K.; Van den Broek, M.; Kostka, S.; Kraft, R.; Soza, A.; Schmidtke, G.; Kloetzel, P.M.; Groettrup, M. Overexpression of the proteasome subunits LMP2, LMP7, and MECL-1, but not PA28 alpha/beta, enhances the presentation of an immunodominant lymphocytic choriomeningitis virus T cell epitope. *J. Immunol.* **2000**, *2000. 165*, 768–778. [CrossRef]
51. Strehl, B.; Joeris, T.; Rieger, M.; Visekruna, A.; Textoris-Taube, K.; Kaufmann, S.H.; Kloetzel, P.-M.; Kuckelkorn, U.; Steinhoff, U. Immunoproteasomes are essential for clearance of Listeria monocytogenes in nonlymphoid tissues but not for induction of bacteria-specific CD8+ T cells. *J. Immunol.* **2006**, *177*, 6238–6244. [CrossRef] [PubMed]
52. Kemball, C.C.; Harkins, S.; Whitton, J.L. Enumeration and Functional Evaluation of Virus-Specific CD4+ and CD8+ T Cells in Lymphoid and Peripheral Sites of Coxsackievirus B3 Infection. *J. Virol.* **2008**, *82*, 4331–4342. [CrossRef] [PubMed]
53. Kemball, C.C.; Harkins, S.; Whitmire, J.K.; Flynn, C.T.; Feuer, R.; Whitton, J.L. Coxsackievirus B3 Inhibits Antigen Presentation In Vivo, Exerting a Profound and Selective Effect on the MHC Class I Pathway. *PLOS Pathog.* **2009**, *5*, e1000618. [CrossRef] [PubMed]
54. Li, J.; Basler, M.; Alvarez, G.; Brunner, T.; Kirk, C.J.; Groettrup, M. Immunoproteasome inhibition prevents chronic antibody-mediated allograft rejection in renal transplantation. *Kidney Int.* **2018**, *93*, 670–680. [CrossRef] [PubMed]
55. Luo, H. Interplay between the virus and the ubiquitin–proteasome system: Molecular mechanism of viral pathogenesis. *Curr. Opin. Virol.* **2016**, *17*, 1–10. [CrossRef]
56. Chen, S.-C.; Chang, L.-Y.; Wang, Y.-W.; Chen, Y.-C.; Weng, K.-F.; Shih, S.-R.; Shih, H.-M. Sumoylation-promoted Enterovirus 71 3C Degradation Correlates with a Reduction in Viral Replication and Cell Apoptosis. *J. Boil. Chem.* **2011**, *286*, 31373–31384. [CrossRef]
57. Basler, M.; Claus, M.; Klawitter, M.; Goebel, H.; Groettrup, M. Immunoproteasome Inhibition Selectively Kills Human CD14+ Monocytes and as a Result Dampens IL-23 Secretion. *J. Immunol.* **2019**, *203*, 1776–1785. [CrossRef]
58. Singh, P.K.; Fan, H.; Jiang, X.; Shi, L.; Nathan, C.F.; Lin, G. Immunoproteasome beta5i-Selective Dipeptidomimetic Inhibitors. *Chem. Med. Chem.* **2016**, *11*, 2127–2131. [CrossRef]
59. Stewart, A.K.; Rajkumar, S.V.; Dimopoulos, M.A.; Masszi, T.; Špička, I.; Oriol, A.; Hájek, R.; Rosiñol, L.; Siegel, D.S.; Mihaylov, G.G.; et al. Carfilzomib, Lenalidomide, and Dexamethasone for Relapsed Multiple Myeloma. *N. Engl. J. Med.* **2015**, *372*, 142–152. [CrossRef]
60. Richardson, P.G.; Sonneveld, P.; Schuster, M.W.; Irwin, D.; Stadtmauer, E.A.; Facon, T.; Harousseau, J.-L.; Ben-Yehuda, D.; Lonial, S.; Goldschmidt, H.; et al. Bortezomib or High-Dose Dexamethasone for Relapsed Multiple Myeloma. *New Engl. J. Med.* **2005**, *352*, 2487–2498. [CrossRef]
61. Hasinoff, B.B.; Patel, D. Myocyte-Damaging Effects and Binding Kinetics of Boronic Acid and Epoxyketone Proteasomal-Targeted Drugs. *Cardiovasc. Toxicol.* **2018**, *18*, 557–568. [CrossRef] [PubMed]

Curriculum vitae

Mein Lebenslauf wird aus datenschutzrechtlichen Gründen in der elektronischen Version meiner Arbeit nicht veröffentlicht

Publication list

2021

Goetzke CC, Althof N, *Neumaier HL*, Heuser A, Kaya Z, Kespohl M, Klingel K, Beling A

Basic Research in Cardiology. 2021 Feb 1;116(1):7.
doi: 10.1007/s00395-021-00848-w.
IF: 6,470

„Mitigated viral myocarditis in A7J mice by the immunoproteasome inhibitor ONX 0914 depends on inhibition of systemic inflammatory responses in CoxsackievirusB3 infection“

2020

Bockstahler M, Fischer A, Goetzke CC, *Neumaier HL*, Sauter M, Kespohl M, Müller AM, Meckes C, Salbach C, Schenk M, Heuser A, Landmesser U, Weiner J, Meder B, Lehmann L, Kratzer A, Klingel K, Katus HA, Kaya Z, Beling A

Circulation. 2020 Jun 9;141(23):1885-1902.
doi: 10.1161/CIRCULATIONAHA.119.043171.
IF: 23,054

„Heart-Specific Immune Responses in an Animal Model of Autoimmune-Related Myocarditis by an Immunoproteasome Inhibitor and Genetic Ablation“

- -

Neumaier HL, Harel S, Klingel K, Kaya Z, Heuser A, Kespohl M, Beling A

Cells. 2020 Apr 28;9(5):1093.
doi: 10.3390/cells9051093.
IF: 5,656

„ONX 0914 Lacks Selectivity for the Cardiac Immunoproteasome in CoxsackievirusB3 Myocarditis of NMRI Mice and Promotes Virus-Mediated Tissue Damage“

Acknowledgments

This dissertation is the cumulation of more than 2,5 years of (experi)mental work for not only me, but many others as well. Thank you first and foremost to everyone at the Beling lab, who supported, helped, laughed with (and at) me during that time. Some of you have become life-long friends and I'm grateful to have met and worked with you! Prof. Antje Beling provided me with the opportunity for this project and with guidance along the way — thank you for your input and for challenging me.
It takes time to do experimental research and so, to my friends and family: I am grateful for your understanding and patience during all of it. Mom and Dad, thank you for your support and always being behind me in everything I do. Claudia and Julia, I truly don’t know how I would do anything without you and your friendship (and the occasional kick in the butt).